Journal of Quantitative Spectroscopy & Radiative Transfer 316 (2024) 108902

Contents lists available at ScienceDirect

Journal of Quantitative Spectroscopy and Radiative Transfer

journal homepage: www.elsevier.com/locate/jqsrt

Empirical rovibrational energy levels for nitrous oxide

Jonathan Tennyson [a,b,*], Tibor Furtenbacher [c], Sergei N. Yurchenko [a], Attila G. Császár [c,d]

[a] Department of Physics and Astronomy, University College London, Gower Street, London WC1E 6BT, UK
[b] Institute for Nuclear Research (ATOMKI), H-4001 Debrecen, Hungary
[c] HUN-REN–ELTE Complex Chemical Systems Research Group, H-1117 Budapest, Pázmány Péter sétány 1/A, Hungary
[d] Laboratory of Molecular Structure and Dynamics, Institute of Chemistry, ELTE Eötvös Loránd University, H-1117 Budapest, Pázmány Péter sétány 1/A, Hungary

ARTICLE INFO

Keywords:
Rovibrational energy levels
N_2O
MARVEL

ABSTRACT

A survey of the huge number of measured rovibrational transitions of the $^{14}N_2{}^{16}O$ isotopologue of nitrous oxide is performed which either confirms the positions, the assignments, and the uncertainties of the measurements or refutes at least one of them. Data from 95 literature sources are analyzed and their assignments adjusted to a uniform set of polyads and associated counting numbers. This is an important result of the present study and this canonical set of vibrational state assignments is recommended for future studies. The adjusted list of 67 930 transitions (43 246 unique ones) then underwent a thorough MARVEL (Measured Active Rotational–Vibrational Energy Levels) analysis, yielding 17 561 empirical rovibrational energy levels. Uncertainties for these levels are determined using a newly implemented bootstrap approach. The bootstrap uncertainties indicate that the uncertainties for about 1.5% of the energy levels had to be increased significantly, often by more than 10 times compared to previous level uncertainty estimates. This study yields empirical values for 78 band origins of $^{14}N_2{}^{16}O$ for states with $\ell = 0$, where ℓ is the vibrational angular momentum quantum number. The measured transitions and the empirical energy levels are compared to the SISAM and the recent NOSL-296 line lists with the result that while the overall agreement is good, there are still a number of issues requiring further careful experimental and modeling studies.

1. Introduction

Nitrous oxide, commonly known as laughing gas due to its medical applications in surgery and dentistry, is a linear asymmetric triatomic molecule with the formula N_2O. N_2O is a trace atmospheric species on Earth, whose atmospheric concentration has been slowly growing in recent decades and it is thought to be a current major remaining destroyer of stratospheric ozone [1]. N_2O has been proposed as an observable species in Earth-like exoplanets [2] and its spectrum has been considered as a possible bio-signature [3]. Therefore, N_2O is included in the list of target species in exoplanet characterization missions [4,5].

The rotation–vibration spectrum of the linear N_2O molecule has been thoroughly investigated [6–180]. These studies often addressed issues related to the atmospheric presence of N_2O and also involved fundamental questions related to the dynamics and spectroscopy of the molecule itself. High-accuracy studies of the spectra of N_2O have also played an important role in providing infrared frequency calibration standards [20,62,66,68–70,84,108].

This work concentrates on the main isotopologue of nitrous oxide, $^{14}N_2{}^{16}O$. There have been many experimental studies of the spectrum of $^{14}N_2{}^{16}O$ yielding high-resolution (rotationally-resolved) data that could be used during the present study. There are a similarly large number of papers [8,11,13–16,19,21,25,26,29,34–37,39–42,45,47,48,50,52,53,61,62,65,75,76,78,79,83,84,86–92,94–96,98,103,104,106,109,112,115,117,121–123,126,130,131,135,138,139,143,144,147,149,151,152,154,160–163,165–167,171,172,177] which do not provide transition data on N_2O of direct use for the present study. Importantly, some of these papers provide line list compilations, both (semi-)empirical ones [125,151,179,181,182] and those based on the use of variational nuclear-motion calculations [177]. The most recent line list relevant for the present study is NOSL-296 [179], which was published while this work was nearing completion.

There are a number of theoretical studies, performed at various levels of sophistication, related to the representation of the potential energy surface [183–189] and the (ro)vibrational spectra [177,188,190–192] of nitrous oxide. These studies, the best of which yield a very large set of rovibrational energies, though with relatively large discrepancies with respect to the experimental information, and enormous line lists, are important to understand the rotational–vibrational spectroscopy of N_2O and, in particular, the ordering of its vibrational states.

* Corresponding author at: Department of Physics and Astronomy, University College London, Gower Street, London WC1E 6BT, UK.
E-mail address: j.tennyson@ucl.ac.uk (J. Tennyson).

https://doi.org/10.1016/j.jqsrt.2024.108902
Received 1 August 2023; Received in revised form 8 January 2024; Accepted 8 January 2024
Available online 19 January 2024

At the beginning of the project described here, we collected all the experimental rovibrational transitions data available for $^{14}N_2{}^{16}O$, with the available assignments and uncertainties, and placed them into a database. This initial phase identified issues with bands given different vibrational assignments in different papers. It was therefore necessary to develop a unique set of vibrational labels to allow the data to be processed. Following this relabeling, a spectroscopic network [193–195] was formed from the lines observed. This allowed the validation of the vast majority of the measured transitions. Occasionally, the same procedure allowed the identification of conflicting or incorrect measurements. After the survey of the measured transitions and the cleansing of the database, we calculated empirical rovibrational energies for the states involved in the measured transitions with the help of the latest version of the Measured Active Rotational–Vibrational Energy Levels (MARVEL) algorithm and code [193,195–197]. The set of measured transitions and the empirical rovibrational energy levels obtained are made available in the Supplementary Information accompanying this paper. The empirical rovibrational energy levels deduced at the end of this study are compared to previous literature results [125,179], revealing several issues.

2. Theoretical details

2.1. MARVEL

The MARVEL algorithm, used extensively during this study, is based on the theory of spectroscopic networks (SN) [193–195]. The SN of a molecule is a graph $G(V, E)$, in which the vertex set V represents the discrete quantum states of the molecule, and the edge set E corresponds to (allowed) transitions between the quantum states. When a large number of accurately measured and assigned, interconnected transitions are available for a given isotopologue of a molecule, MARVEL yields empirical rovibrational energies for the V set.

The latest version of the MARVEL code, based on the MARVEL algorithm, is used to obtain empirical rotational–vibrational energy levels of $^{14}N_2{}^{16}O$, all characterized with well-defined uncertainties. The energies and the uncertainties of the V set are derived from a collection of previously measured [6,7,9,10,12,17,18,22–24,27,28,30–33,38,43,44,46,49,51,54–60,63,64,66–74,77,80–82,85,93,97,99–102,105,107,108,110,111,113,114,116,118–120,124,125,127–129,132–134,136,137,140–142,145,146,148,150,153,155–159,164,168–170,173–176,178] rotational-vibrational transitions with appropriate labels and uncertainties. Note that the uncertainties of the empirical energies reflect not only the accuracy of the individual measurements but also the topology of the SN; for example, how the most accurately determined transitions are connected.

2.2. Labeling

Low-lying vibrational states of semirigid molecules can be characterized using the standard harmonic oscillator (HO) notation [198]. In the case of the N_2O molecule, the standard way to denote the fundamentals is as follows: ν_1 (NO stretch), with a harmonic/anharmonic wavenumber of 1298/1285 cm^{-1}, ν_2 (degenerate bend), with wavenumbers close to 596/590 cm^{-1}, and ν_3 (NN stretch), at 2282/2224 cm^{-1} [83,190]. Upon excitation of the ν_2 mode, the bendings in the two, orthogonal planes can have different phases. Thus, an angular momentum arises as if the bent molecule rotated about the molecular axis. This so-called vibrational angular momentum quantum number, ℓ, takes positive values with $\ell = v_2, v_2 - 2, v_2 - 4, \ldots$. Therefore, the vibrational states could be labeled as $(v_1 v_2^{\ell} v_3)$; thus, the label for the vibrational ground state is $(v_1 v_2^{\ell} v_3) = (00^0 0)$.

The (harmonic and anharmonic) vibrational fundamentals obey the approximate relationship $\nu_3 \approx 2\nu_1 \approx 4\nu_2$. These relationships lead to many resonances among the excited vibrational states of $^{14}N_2{}^{16}O$, meaning that they are best represented using a polyad notation $(P\,\ell\,N)$ [199,200], whereby the polyad number P is given by

$$P = 2v_1 + v_2 + 4v_3 \tag{1}$$

and N is the polyad counting number (the best way of defining N is discussed below). In addition, states with $\ell > 0$ can occur with both 'e' and 'f' rotationless parity, while those with $\ell = 0$ only correspond to 'e' states. Finally, all states are characterized by a total angular momentum quantum number, J, which has to satisfy $J \geq \ell$ for a given vibrational state. A surprising number of sources contained lines assigned to states with $J < \ell$. These lines were all removed from further analysis during the initial phase of our study.

Note that from this set of labels the only rigorous quantum numbers are J and the rotationless parity p; these also give the total parity as $(-1)^{J+p}$, where $p = 0$ for 'e' states and 1 for 'f' states. In what follows, rovibrational states are labeled with the quintuplet $(P\,\ell\,N\,p\,J)$, with p = e/f.

While in principle it is straightforward to assign vibrational states to a given polyad, from about $P > 10$ the number of cases with significant interpolyad interactions [175,178] increases, which leads to resonances between states with different polyad numbers. Allocation of counting numbers N to vibrational states is also complicated. For states with $\ell = 0$ there is reasonable agreement in the literature about the appropriate counting numbers for particular vibrational bands. However, this is not true for states with $\ell > 0$, which show significant variation on the choice of N for the same state between different sources; these variations are particularly marked for states with $\ell = 2$.

In order to achieve a unique set of quantum numbers, required for the derivation of empirical energies *via* a MARVEL analysis, we adopted a two-step procedure. In order to be able to process the data successfully we grouped bands according to the stated band origins, adopting the value of N most commonly used in the literature. Once the complete transition set had been assembled and validated, we then renumbered all the polyads assuming that the lowest vibrational state for each (P, ℓ) combination was labeled $N = 1$, that states with $\ell \geq 1$ had a single band origin for the (quasi)-degenerate 'e/f' pair, and allowance was made for so-far unobserved vibrational levels. To get a master set we used the recent 'Ames' variational nuclear motion calculations of Huang et al. [177]. For this purpose we simply used the computed energy levels to give the lowest energy level for each vibrational band and then determined counting numbers from this list. The polyad number P for a given vibrational band, for which there were no disagreements between different experimental papers, were retained. This method avoided relying on quantum number assignments from either of the two variational nuclear motion calculations [177,201] we considered during this project; such assignments are also known to have difficulties for higher vibrational states and, indeed, the two studies do not always agree.

We note that these variational calculations do not actually give vibrational band origins for states with $\ell \geq 1$ as the $J = 0$ state is unphysical for these vibrational states; in this case we used the lowest 'e' level with $J = \ell$ for a given vibrational band. In practice, we found that the above procedure gave a canonical numbering scheme, which we provide below, without any significant problems or ambiguities. The full set of vibrational state labels with vibrational band origins and/or lowest state energies plus associated polyad and counting numbers are given in the Supplementary Material. We suggest that this numbering scheme should be adopted for future studies of the spectroscopy of N_2O.

2.3. Uncertainty quantification of energy levels: a bootstrap approach

It is important to transfer the (supposedly high) accuracy of high-resolution spectroscopic line-center measurement results to the empirical energy values derived through MARVEL. Due to issues one can legitimately raise with respect to the accuracy of many of the line uncertainties reported in experimental high-resolution spectroscopic

Table 1
Two examples illustrating how the bootstrap method applied works in determining uncertainties, with 95% confidence intervals, of empirical energy levels.

Energy level ($P\ell N$ e/f J)	MARVEL energy /cm^{-1}	Original unc. /cm^{-1}	Bootstrap unc. /cm^{-1}	Tag of line	Initial unc. /cm^{-1}	Predicted energy /cm^{-1}
(17 1 14 e 36)	10 425.772	0.001	0.028	16KaCaKaPe.1421	0.001	10 425.772
				04BeCaPeTa.409	0.005	10 425.814
(16 2 10 e 25)	9374.588	0.001	0.022	22KaTaKaCab.2193	0.001	9374.588
				04BeCaPeTa.84	0.005	9374.635
				04BeCaPeTa.85	0.005	9374.634

investigations, the uncertainty associated with the empirical rovibrational energy levels must be determined with special care. There are cases where one can even question the true meaning of the uncertainty of an empirical energy level. In this study, we utilize a bootstrap method [202,203] to derive the final uncertainties of the empirical energy levels. In what follows we briefly explain why we switched from our previous best practice [204] to the bootstrap technique.

We have been testing various methods of generating uncertainties using the Marvel procedure, including a robust method advocated by Watson [205], and the processing of transitions in segments, based on their claimed uncertainty [204] (this type of uncertainty is called here and later the *original* uncertainty). To obtain a self-consistent spectroscopic database, in all previous Marvel-based studies it has proved necessary to manually increase the uncertainties of some of the measured transitions. Nevertheless, choosing the transitions for which the stated uncertainty needs to be increased is far from being straightforward. The principal reason for this is that the precision with which initial uncertainties are given by experimental spectroscopists can often be questioned. For example, it is easy to imagine cases where Marvel leaves unchanged a relatively inaccurate measurement result because an overly-optimistic initial uncertainty was assigned to it and increases the uncertainty of a more accurate transition whose uncertainty was estimated pessimistically. As a result, even if several measurements are available the quantum state may become characterized by an incorrect energy value and an incorrect uncertainty. Unfortunately, without detailed knowledge of the measured spectra (actual spectra are very rarely published as supplementary material to spectroscopic papers), it is almost impossible to determine whether the initial uncertainties are optimistic or perhaps pessimistic; thus, this source of error is almost always present during a Marvel-type joint analysis of the complete set of measured transitions. The only thing one can do is to increase the uncertainty of the energy levels where Marvel has the chance, or even a tendency, to make an incorrect choice.

"Bootstrap" approaches [202,203] are suitable to obtain reasonable uncertainties in the case of conflicting measurements, where without this approach too small uncertainties would be given for energy levels if some of the measurement results were rejected. The variant of the bootstrap procedure we use is as follows: bootstrap samples are generated by multiplying the uncertainty of each transition by a random number between 1 and 10, and then we rerun Marvel for each sample. After a hundred or more such runs, we check whether the average of the bootstrapped energies is different from the original Marvel energy. If the energies calculated by the two methods differ by a prescribed amount, the uncertainty of the Marvel energy is increased. If the energies calculated by the two methods are close but the standard deviation of the bootstrap energies is larger than the uncertainty of the original Marvel energy, the uncertainty of the Marvel energy will also be increased.

To illustrate how our version of the bootstrap method works, we present in Table 1 results for the two quantum states for which the ratio of the bootstrap uncertainty to the original uncertainty is the largest. The first quantum state, $(P\ell N\,\mathrm{e/f}\ J) = (17\ 1\ 14\ e\ 36)$, is determined by two measured transitions, 16KaCaKaPe.1421 [150] and 04BeCaPeTa.409 [123]. The difference between the two predicted energy values is as large as 0.042 cm^{-1}, significantly larger than the reported experimental uncertainty of either line. Since the original uncertainty of the supposedly more accurately measured transition is five times smaller than that of the other one, Marvel increased the uncertainty of the second transition. However, without actually seeing the original spectra, it is impossible to decide whether the initial uncertainty of 16KaCaKaPe.1421 [150] is too optimistic or not. This line can be very weak, or saturated, or may also be subject to other measurement issues; therefore, based on the available experimental results the 0.001 cm^{-1} measurement uncertainty is too small. The bootstrap method detects the inconsistency between the predicted energy values and significantly increases the original uncertainty determined by Marvel, reflecting better the present situation. In the second case, the energy of the (16 2 10 e 25) state is determined by three measured transitions coming from two sources [123,175]. Two of the transitions, coming from the same but older source, 04BeCaPeTa [123], predict the same empirical energy, but the third transition, with the smallest initial uncertainty from a very recent source, 22KaTaKaCab [175], predicts an energy value different by as much as 0.04 cm^{-1}. Thus, we are faced with the 'philosophical' question which measurements and which sources are more reliable. Unfortunately, without seeing the measured but unpublished spectra it is impossible to decide whether the stand-alone recent measurement, with lower uncertainty, or the transitions which are perceived to be less accurate but confirm each other are more accurate. If one were to accept the literature results, the lower-uncertainty choice would determine the energy value of the quantum state; therefore, Marvel increased the uncertainties of the two other transitions. However, if the transition assumed to be the best is not as good as claimed by its 'original' uncertainty, we end up with an energy value with a much too small associated uncertainty. The bootstrap approach solves the dilemma by providing a significantly increased uncertainty for the energy level. Given the data available, this appears to be the better choice and the uncertainties reported in the Supplementary Material for the empirical energy levels were obtained with our version of the bootstrap technique.

3. Results and discussion

3.1. Data sources

During this study, a concerted effort was made to collate *all* measured and assigned rovibrational transitions of the $^{14}N_2{}^{16}O$ molecule available in the literature. The number of rovibrational transitions collected from the literature, based on 91 sources [6,7,9,10,12,17,22,27,30–33,38,43,44,46,49,51,54–60,63,64,66–74,77,80–82,85,93,97,99–102,105,107,108,110,111,113,114,116,118–120,123–125,127–129,132–134,136,140–142,145,146,148,150,153,155–159,164,168–170,173–176,178,180], is 67 930. We were able to validate 66 707 of these transitions *via* a detailed Marvel-based analysis and a systematic check against the very recent variational nuclear motion calculations of Zobov et al. [201]. This check led to the removal of a small number of transitions which were inconsistent with these calculations. It is important to note that if a transition is not part of the principal component of the spectroscopic network of $^{14}N_2{}^{16}O$, we are not able to validate it. It is impressive that these experimental studies involved altogether 174 vibrational bands.

Some older sources, including 61RaWiRaEa [18], 64PlTiMa [24], 64Pliva [23], and 68Plivaa [28], were considered insufficiently accurate to be included in the compilation of transitions data used during

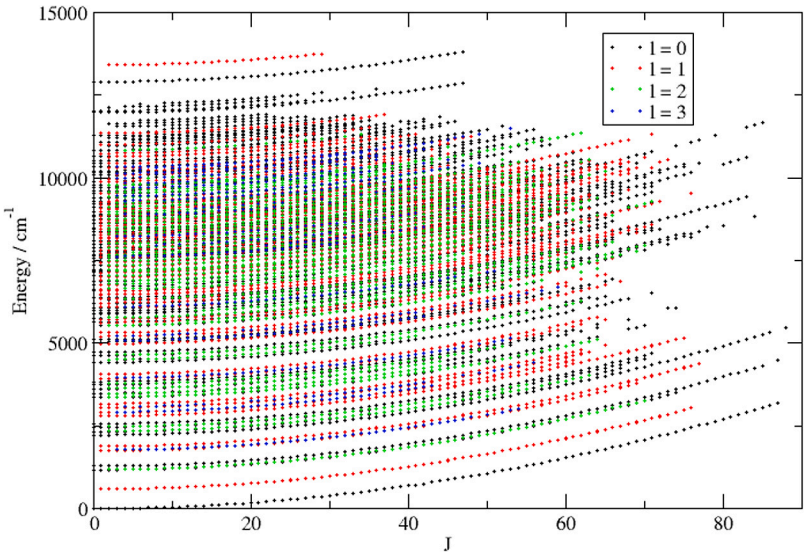

Fig. 1. Overview of the energy levels determined in this work designated by the ℓ and J quantum numbers.

the MARVEL analysis. We were unable to obtain a copy of the source 09SuDiZo [137].

Some of the older sources either explicitly mention that calibration is an issue, *e.g.*, 50HeHe [7], or subsequent studies have identified the need for recalibration, *e.g.*, for 82Guelachv [63]. Therefore, we tested a number of sources against the other available data to see which required recalibration. In the end, we recalibrated three data sets: the wavenumbers due to 50HeHe [7], 82Guelachv [63], and 95CaPeBaTe [93] were scaled by calibration factors of 0.999 998 11, 0.999 999 890, and of 1.000 003 08, respectively. Somewhat detailed notes on various sources are given in Appendix A to this paper.

The experimental sources used to construct the $^{14}N_2{}^{16}O$ spectroscopic network of this study are listed in Table 2. Table 2 also contains the information how many transitions have been validated and how many transitions we had to delete from each source (see the available(A) / validated(V) / deleted(D) column). The *AOU* (average original uncertainty) column shows the average of the measurement uncertainty of the given source and the values of *AMR* (average MARVEL reproduction) shows how well, in an average sense, the empirical (MARVEL) energy levels are able to reproduce the experimentally measured lines of the given source. The last column of Table 2, *MR*, shows the maximum reproduction of the given source, *i.e.*, the largest difference between the experimentally measured wavenumber and the transition predicted by MARVEL. For most sources all measured transitions have been validated. Nevertheless, we did identify a number of incompatibilities in between some of the sources, which led us to delete a number of lines. The largest number of deleted transitions, 121, 112, and 88 concern the sources 60TiPlBe [17], 06HePiGuSo [128], and 50HeHe [7], respectively. It is noteworthy that for 60TiPlBe [17] this means that almost one fourth of the measured lines in the infrared region had to be deleted.

The SN of $^{14}N_2{}^{16}O$ has a single principal component. This is due to the rigidity of the NN unit. Altogether, out of the 67 930 transitions considered, we could validate 66 707, all belonging to the principal component. 635 transitions, which should belong to the principal component, were removed during our MARVEL analysis. While some of these transitions have been misassignments (or have $J < \ell$), most were removed on the ground of accuracy. The remaining 616 transitions belong to 167 floating components; we did not make an attempt to attach these to the principal component of the SN of $^{14}N_2{}^{16}O$. It is also worth emphasizing that among the 67 930 transitions considered there are only 43 246 unique ones. This means that a significant number of transitions have been measured more than once; in fact, the number of transitions measured just one time is 27 444, while there are 4 and 142 transitions which were measured 7 and 6 times, respectively (the number of empirical rovibrational energy levels determined, 17 561, is significantly closer to 43 000 than to 68 000).

Note also that in SNs the degrees of the energy levels display an inverse-power-law-like distribution [194,195], implying the presence of a small number of high-degree quantum states, called hubs, in the SN. The highest-degree hubs of $^{14}N_2{}^{16}O$ have the general label (0 0 1 e J) with $J = 11, 12, 13, 15, 16, 17$, and 18, and these vertices have as many as 500 connecting edges each. This means that if hubs are defined as the top 1% of the vertices with the highest degrees (this translates to 174 hubs for the present dataset), than slightly more than 60% of the transitions are connected to less than 1% of the vertices (apart from a diminishing number of exceptions, hubs are the lower states of the measured transitions). These observations are of interest especially for future high-resolution and precision-spectroscopy experiments, including those aiming at the presently readily available accuracy of a few kHz [206–208] rather than several MHz.

Fig. 1 shows the distribution of the 17 561 empirical energy levels determined as a function of the J rotational quantum number. To provide additional information, the states with different ℓ values are indicated with different colors. As seen in Fig. 1, our network includes levels with $\ell \leq 3$. In practice, 01BaVe [113] and 22KaTaKaCaa [174] contain a combined total of 223 transitions to states with $\ell = 4$ and 01BaVe [113] gives 224 transitions to states with $\ell = 5$, meaning that all but two of the transitions not attached to the principal component are associated with states with $\ell > 3$.

3.2. Level uncertainties

As mentioned in Section 2.3, in this study we employed a method new to MARVEL, called bootstrap, which does not alter the uncertainties of the measured transitions but improves the uncertainties of the empirical (MARVEL) energy levels. The bootstrap approach applied can only increase the uncertainties.

Fig. 2 shows the ratio of the 'bootstrap' and the 'original' uncertainties of the empirical rovibrational energy levels. In most cases, the bootstrap algorithm barely raises the original MARVEL uncertainties. In 92% of cases the ratio is less than 5 and in only 1.5% of cases the ratio is larger than 10. These numbers suggest that the 'original' uncertainty estimation employed within MARVEL is a good approximation in most cases, but in about 1-2% of the cases it is necessary to increase the uncertainty of the empirical energy levels significantly. The ratio above

Table 2
Experimental sources used to construct the $^{14}N_2{}^{16}O$ rovibrational spectroscopic network of this study. The data given include, for each source, the wavenumber ranges of the validated transitions (in cm^{-1}), the number of actual (*A*), validated (*V*), and deleted (*D*) transitions, and selected uncertainty statistics (in cm^{-1}), where *AOU* = average original uncertainty, *AMR* = average MARVEL reproduction of the source's lines, and *MR* = maximum reproduction in the source. RC (in the tag) = recalibrated source (see text).

Segment tag	Range	*A*/*V*/*D*	*AIU*	*AMR*	*MR*
78ReMeDy [58]	0.002–0.009	3/3/0	5.00×10^{-9}	1.10×10^{-12}	5.00×10^{-9}
64LaLi [22]	0.835–2.521	4/4/0	2.67×10^{-6}	3.60×10^{-7}	3.34×10^{-6}
47CoElGo [6]	0.838–0.838	1/1/0	3.34×10^{-6}	1.34×10^{-7}	3.34×10^{-6}
75CaKu [51]	0.838–0.838	1/1/0	2.07×10^{-8}	2.40×10^{-11}	2.07×10^{-8}
75Bogey [49]	1.662–4.156	4/4/0	4.59×10^{-6}	2.84×10^{-6}	8.34×10^{-6}
52Tetenbau [10]	1.676–1.676	1/1/0	3.34×10^{-6}	1.20×10^{-5}	1.20×10^{-5}
70ScMuLa [32]	1.676–2.514	2/2/0	3.50×10^{-7}	7.34×10^{-9}	4.34×10^{-7}
71LeHoThMa [33]	2.504–2.519	5/4/1	3.34×10^{-6}	3.87×10^{-7}	3.34×10^{-6}
51JoTrGo [9]	3.352–4.190	2/2/0	9.17×10^{-6}	1.07×10^{-6}	1.00×10^{-5}
56BuGo [12]	3.352–10.055	9/9/0	1.33×10^{-5}	5.45×10^{-6}	2.00×10^{-5}
70PeSuFr [30]	4.172–10.082	35/34/1	2.64×10^{-6}	1.50×10^{-6}	1.60×10^{-5}
18LaScAgMe [157]	5.028–5.866	2/2/0	4.00×10^{-6}	2.60×10^{-6}	4.36×10^{-6}
68FrAr [27]	5.028–5.028	1/1/0	6.67×10^{-6}	1.83×10^{-6}	6.67×10^{-6}
14TiChChCh [146]	6.676–2272.183	219/212/0	1.17×10^{-6}	2.03×10^{-7}	1.01×10^{-5}
74BuVaGeKa [43]	10.055–15.918	6/6/0	1.67×10^{-6}	3.62×10^{-7}	1.67×10^{-6}
76AnBuKaKr [56]	12.568–18.518	97/97/0	7.50×10^{-7}	8.04×10^{-8}	3.04×10^{-6}
06DrMa [127]	20.103–55.230	72/71/0	2.50×10^{-6}	6.81×10^{-7}	7.58×10^{-6}
90Yamada [82]	20.103–47.637	32/32/0	1.00×10^{-4}	7.18×10^{-5}	1.64×10^{-4}
03MoYa [120]	20.940–21.776	2/2/0	5.00×10^{-8}	2.05×10^{-9}	5.34×10^{-8}
97MoFaTaYa [102]	20.940–24.285	5/5/0	6.67×10^{-7}	1.40×10^{-6}	1.78×10^{-6}
99MoYaMa [108]	20.862–26.081	60/60/0	6.87×10^{-7}	2.41×10^{-7}	5.80×10^{-6}
89VaJeWeMa [80]	50.129–50.241	3/3/0	6.67×10^{-6}	7.52×10^{-7}	6.67×10^{-6}
83JoKaHo [64]	542.456–645.418	355/355/0	4.00×10^{-5}	1.28×10^{-4}	6.79×10^{-4}
07Horneman [132]	542.920–635.235	533/509/24	1.74×10^{-5}	2.26×10^{-5}	2.26×10^{-3}
92TaLoLu [85]	554.029–619.385	241/241/0	5.00×10^{-5}	1.01×10^{-4}	1.20×10^{-3}
96WeSiRe [101]	557.231–615.994	96/96/0	6.00×10^{-4}	1.27×10^{-4}	6.00×10^{-4}
04Toth [125]	577.760–7232.274	1121/1121/0	5.00×10^{-4}	1.25×10^{-4}	3.33×10^{-3}
89MaWeVa [77]	896.945–989.668	18/18/0	1.74×10^{-4}	6.89×10^{-5}	3.34×10^{-4}
96TaEvZiMa [100]	897.010–1074.417	129/129/0	1.67×10^{-7}	9.99×10^{-8}	2.22×10^{-6}
87Toth [73]	900.926–2392.452	1207/1196/0	6.00×10^{-5}	3.27×10^{-5}	9.44×10^{-4}
72SoJa [38]	922.423–956.347	27/27/0	1.95×10^{-4}	9.13×10^{-4}	1.12×10^{-3}
75WhSuRiHa [54]	925.982–970.092	33/33/0	8.34×10^{-7}	1.45×10^{-6}	3.80×10^{-6}
87ZiWeMa [74]	1037.189–1084.591	9/9/0	1.59×10^{-4}	4.86×10^{-5}	2.67×10^{-4}
85WeJeHiMu [70]	1104.849–1914.718	32/31/0	2.81×10^{-4}	1.63×10^{-4}	7.98×10^{-4}
86Toth [71]	1104.791–1348.351	1061/1047/0	6.00×10^{-5}	4.40×10^{-5}	6.46×10^{-4}
82Guelachv_RC [63]	1118.129–1342.938	649/649/0	5.00×10^{-5}	1.10×10^{-4}	9.99×10^{-4}
84Toth [67]	1133.468–1236.586	54/54/0	2.00×10^{-4}	2.80×10^{-4}	7.83×10^{-4}
85BrTo [68]	1132.024–4749.125	240/240/0	6.00×10^{-5}	5.93×10^{-5}	2.58×10^{-4}
15GaCaCoFa [148]	1161.479–1161.479	1/1/0	3.00×10^{-7}	1.49×10^{-7}	3.00×10^{-7}
18AlLaGaLa [156]	1245.765–1309.847	73/73/0	2.69×10^{-5}	8.41×10^{-6}	1.36×10^{-4}
21HjGeKrHu [168]	1251.600–1318.138	179/179/0	8.07×10^{-6}	5.67×10^{-6}	2.39×10^{-4}
85WeHiMa [69]	1257.316–1339.843	14/14/0	1.57×10^{-4}	1.24×10^{-4}	4.65×10^{-4}
87HiWeMa [72]	1257.509–1335.006	28/24/4	1.69×10^{-4}	1.97×10^{-4}	1.97×10^{-3}
80NaKaYaHa [60]	1295.476–1311.284	4/4/0	5.25×10^{-4}	4.77×10^{-4}	9.13×10^{-4}
89VaScWeMa [81]	1591.326–1672.707	8/8/0	2.59×10^{-4}	1.21×10^{-4}	3.34×10^{-4}
76AmGu [55]	1831.706–3191.180	3944/3861/77	2.00×10^{-4}	3.81×10^{-4}	5.59×10^{-3}
01BaVe [113]	2044.525–2266.349	3242/3071/7	8.00×10^{-3}	7.27×10^{-4}	6.75×10^{-2}
03BaPiVe [118]	2072.675–2200.925	753/444/1	4.00×10^{-4}	2.46×10^{-4}	3.09×10^{-3}
74FaDu [44]	2098.489–2230.678	997/994/3	3.00×10^{-3}	3.97×10^{-3}	4.07×10^{-2}
76VaLeCaBo [57]	2135.289–2268.099	201/134/67	5.00×10^{-4}	8.89×10^{-4}	8.10×10^{-3}
13KnWiGiRa [145]	2189.273–2213.246	24/24/0	2.67×10^{-5}	1.47×10^{-5}	4.02×10^{-5}
21JiMc [169]	2206.659–2208.093	3/3/0	2.00×10^{-4}	1.39×10^{-5}	2.00×10^{-4}
04NeSuVa [124]	2224.588–2251.574	38/38/0	5.00×10^{-4}	6.92×10^{-5}	5.00×10^{-4}
74KrSa [46]	2267.096–2618.035	1838/1825/13	2.00×10^{-2}	3.22×10^{-3}	5.00×10^{-2}
60TiPlBe [17]	2438.220–3502.620	884/763/121	5.10×10^{-2}	3.03×10^{-2}	1.64×10^{-1}
99Toth [110]	3676.940–7795.203	1328/1328/0	2.78×10^{-4}	5.43×10^{-5}	4.49×10^{-3}
06HePiGuSo [128]	3900.809–4041.312	1011/893/112	1.00×10^{-3}	6.19×10^{-4}	1.50×10^{-2}
84PoPeJeWe [66]	4341.141–4753.311	39/39/0	1.97×10^{-4}	5.79×10^{-5}	4.00×10^{-4}
16WeBrSeWe [153]	4418.202–4439.792	41/41/0	4.66×10^{-5}	3.55×10^{-4}	4.29×10^{-4}
20ZhBaFlHo [164]	4415.014–4415.014	1/1/0	2.00×10^{-5}	4.83×10^{-6}	2.00×10^{-5}
80BrCoCuHo [59]	4607.694–4657.886	64/64/0	1.00×10^{-3}	8.71×10^{-4}	1.48×10^{-3}
06WaPeTaGa [129]	5313.693–8987.678	2356/2356/0	5.96×10^{-3}	3.76×10^{-3}	3.13×10^{-2}
19BeMoKaKa [158]	5696.223–5908.020	2166/2166/0	1.11×10^{-3}	5.65×10^{-4}	3.24×10^{-2}
07LiKaPeTa [134]	5906.331–6832.402	2217/2213/4	1.00×10^{-3}	9.73×10^{-4}	1.76×10^{-2}
07LiKaMaRo [133]	6001.771–6884.882	5094/5072/1	1.42×10^{-3}	1.01×10^{-3}	3.08×10^{-2}
00WeKaCaBa [111]	6436.315–12141.237	3578/3538/40	2.69×10^{-3}	4.39×10^{-3}	6.51×10^{-2}
95CaPeBaTe_RC [93]	6436.313–10832.947	3160/3158/2	5.00×10^{-3}	4.43×10^{-3}	8.92×10^{-2}
19LiWaTaKa [159]	6519.115–6597.240	88/88/0	8.86×10^{-6}	4.21×10^{-6}	5.44×10^{-5}
22Iwakuni [173]	6549.562–6596.114	46/46/0	1.83×10^{-5}	1.40×10^{-5}	8.87×10^{-5}
09LiKaPeHu [136]	6789.852–7065.586	1154/1148/6	1.00×10^{-3}	1.11×10^{-3}	2.21×10^{-2}
12LuMoLiPe [142]	6949.767–7725.398	6226/6191/12	1.00×10^{-3}	6.69×10^{-4}	1.33×10^{-2}
23KaMoTaCa [178]	7250.027–7652.630	3329/3307/0	1.00×10^{-3}	6.11×10^{-4}	3.60×10^{-2}
16KaCaKaPe [150]	7601.172–8329.631	2968/2963/5	1.00×10^{-3}	5.88×10^{-4}	2.72×10^{-2}

(*continued on next page*)

Table 2 (*continued*).

11LiKaPeTa [140]	7647.529–7918.173	1746/1742/4	1.00×10^{-3}	9.13×10^{-4}	2.42×10^{-2}
22KaTaKaCab [175]	7647.527–7988.178	2423/2421/2	1.00×10^{-3}	6.57×10^{-4}	2.36×10^{-2}
99HiQu [107]	7783.475–7788.489	8/8/0	1.00×10^{-3}	1.17×10^{-3}	2.03×10^{-3}
50HeHe_RC [7]	7970.763–12898.443	1148/1060/88	3.00×10^{-2}	3.19×10^{-2}	1.51×10^{-1}
22KaTaKaCaa [174]	8272.503–8619.558	3132/3097/3	8.00×10^{-4}	4.07×10^{-4}	1.66×10^{-2}
21KaKaTaCa [170]	8325.774–8622.078	2745/2745/0	1.00×10^{-3}	5.51×10^{-4}	1.66×10^{-2}
03DiPeTaTe [119]	8836.109–10092.626	719/692/27	3.23×10^{-3}	5.12×10^{-3}	3.44×10^{-2}
04BeCaPeTa [123]	9074.119–9621.037	659/658/1	5.10×10^{-3}	4.55×10^{-3}	5.27×10^{-2}
98GaCaKaSt [105]	9362.110–9419.797	68/68/0	5.37×10^{-3}	1.90×10^{-2}	4.68×10^{-2}
24SiSeEmMa [180]	9842.540–11972.969	235/231/4	4.51×10^{-4}	1.34×10^{-3}	1.48×10^{-2}
02BeKaCa [116]	9910.657–9951.791	22/22/0	1.00×10^{-2}	5.79×10^{-3}	2.45×10^{-2}
01CaWeTaPe [114]	10084.048–12021.132	946/943/3	1.76×10^{-2}	5.09×10^{-3}	9.63×10^{-2}
70Pliva [31]	10756.448–10832.966	134/134/0	1.50×10^{-2}	3.81×10^{-3}	1.64×10^{-2}
22LuGo [176]	11233.770–11283.200	53/53/0	1.02×10^{-2}	8.08×10^{-3}	3.85×10^{-2}
96Campargu [97]	11233.777–12221.945	241/241/0	1.50×10^{-2}	9.71×10^{-3}	6.06×10^{-2}
11MiPeTaCa [141]	12764.164–12899.183	140/140/0	1.00×10^{-2}	4.81×10^{-3}	3.31×10^{-2}
17ZhWaLiZh [155]	12857.786–12898.904	41/41/0	2.82×10^{-3}	6.14×10^{-4}	6.42×10^{-3}

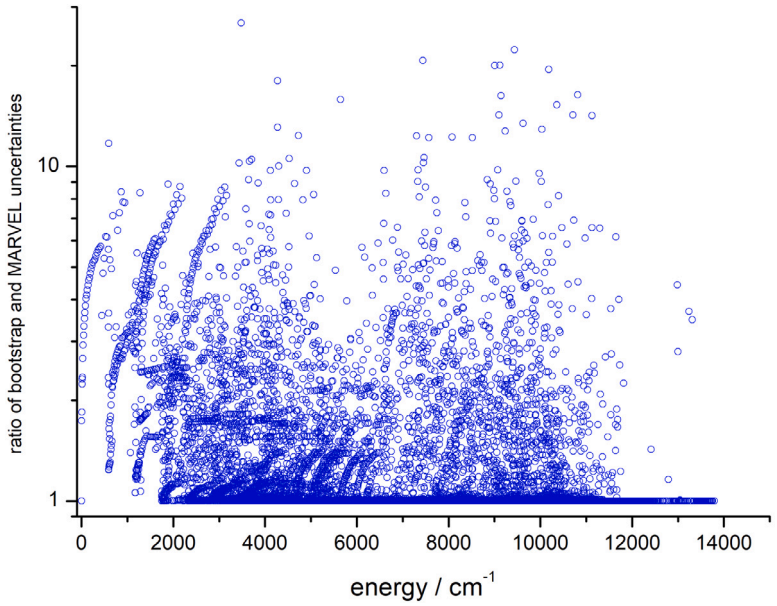

Fig. 2. Ratio of the uncertainties of the empirical rovibrational energy levels of the new bootstrap approach and the traditional Marvel estimates.

about 12 000 cm^{-1} is almost always one. This is due to the fact that the bootstrap approach will only increase the uncertainty if there are more than one (conflicting) measurements available.

3.3. Vibrational bands and band origins

Table 3 summarizes the vibrational bands which could be determined based on the set of measured rovibrational transitions. It is important to note that we use the $\ell = J$ definition for a vibrational band origin (VBO), *i.e.*, where $\ell > 0$, we treat the lowest possible energy level as the VBO. While comparing the 78 VBOs (with $P_{max} = 24$) determined through our Marvel analysis to effective Hamiltonian parameters of 04Toth [125], for the $(P\,\ell\,N) = (1\,1\,1)$ VBO we observed a significant discrepancy. Since this VBO is determined in our Marvel analysis by a single measured transition, taken from 50HeHe [7], and the uncertainty of this band is 0.06 cm^{-1}, we finally did not delete this transition but issue this warning. Future accurate measurements should be able to settle this simple issue.

There are a further number of small but significant discrepancies among the entries of Table 3, on the order of 0.001 cm^{-1}, not discussed here. It is worth pointing out the discrepancies larger than 0.01 cm^{-1}. Such cases include $(P\,\ell\,N) = (11\,1\,7)$, $(12\,2\,6)$, $(13\,1\,7)$, $(15\,1\,9)$, and $(17\,3\,15)$. For $P > 19$ there are significant discrepancies for most states. These deviations require further detailed studies, beyond the scope of the present investigation.

3.4. Empirical rovibrational energy levels

From the 67 930 measured rovibrational transitions (43 246 unique ones) collected we were able to determine 17 561 energy levels from 0 up to 13 790 cm^{-1}. The highest rotational quantum number, J, in our empirical (Marvel) energy-level set is 88, being part of the $(P\,\ell\,N) = (4\ 0\ 1)$ vibrational band. The largest polyad number, P, and polyad counting number, N, are 25 and 28, respectively. We note that 20OgMiMuMu [165] used a novel optical centrifuge technique to measure transitions involving rotational states up to $J = 206$; however, they only actually measured 11 between $J'' = 140$ and $J'' = 205$, so these data could not be used to form a network. The vibrational excitations v_1, v_2, and v_3 range up to 9, 16, and 5, respectively.

We note that coverage of the states with $\ell = 0, 1$, and 2 generally extends to high energy (polyad number). The coverage is more limited for states with $\ell = 3$. While a few transitions involving levels with $\ell = 4$ and 5 have been observed (*vide supra*), these do not connect to the principal component; thus, the empirical energy levels we have determined are limited to those with $\ell \leq 3$.

4. Comparison with previous line lists

This section provides comparisons of our MARVEL-based results with two line lists, namely the SISAM database, called here 04Toth [125], and the very recent Nitrous Oxide Spectroscopic Line List (NOSL-296) [179], designed for atmospheric applications.

Table 3
Summary of the vibrational states of $^{14}N_2^{16}O$ considered in this work. The vibrational states are designated using the polyad-based notation (P, ℓ, N), with $P = 2v_1 + v_2 + 4v_3$, and ℓ and N are the vibrational angular momentum quantum number and the polyad counting number, respectively. The lowest, $J = \ell$, energy level for each vibrational band given by the calculations of Huang et al. [177], denoted Ames, and the empirical, effective Hamiltonian (EH) band origins (with citations), are given in cm^{-1}.

P l N	MARVEL	AMES	EH	P l N	MARVEL	AMES	EH	P l N	MARVEL	AMES	EH
0 0 1	0.0(0)	0.00	0.000 [125]	11 1 8	6571.590(1)	6571.60	6571.590 [125]	15 1 5	8425.849(1)	8425.75	8425.847 [175]
1 1 1	589.606223(7)	589.60	589.606 [125]	11 1 9	6631.431(2)	6631.77	6631.429 [133]	15 1 8	8560.0019(8)	8560.05	8560.000 [150]
2 0 1	1168.13237(2)	1168.13	1168.132 [125]	11 1 10	6773.346(7)	6773.61	6773.348 [134]	15 1 9	8666.974(2)	8667.05	8666.938 [129]
2 0 2	1284.903342(5)	1284.91	1284.903 [125]	11 1 11	6893.051(2)	6893.21	6893.051 [133]	15 1 10	8705.236(1)	8705.82	8702.237 [150]
2 2 1	1180.26532(2)	1180.26	1180.265 [125]	11 1 12	6996.842(2)	6996.94	6996.840 [133]	15 1 11	8708.369(1)	8709.61	8705.366 [150]
3 1 1	1749.9042(4)	1749.90	1749.907 [125]	12 0 1	6580.85352(1)	6580.82	6580.854 [125]	15 1 12	8844.271(1)	8844.56	8844.278 [142]
3 1 2	1881.1003(2)	1881.12	1881.101 [125]	12 0 2	6630.434(2)	6630.39	6630.429 [134]	15 1 14	8960.5835(8)	8960.75	8960.588 [150]
3 3 1	1771.9597(3)	1771.97	1771.960 [125]	12 0 4	6768.502(1)	6768.45	6768.502 [125]	15 1 16	9062.1621(8)	9062.26	9062.158 [142]
4 0 1	2223.7567419(3)	2223.76	2223.757 [125]	12 0 6	6868.5498(2)	6868.52	6868.550 [125]	15 1 17	9186.5218(8)	9187.96	9186.521 [178]
4 0 2	2322.57323(6)	2322.56	2322.573 [125]	12 0 7	6882.691(1)	6882.61	6882.692 [158]	15 3 1	8225.739(2)	8225.72	8225.737 [133]
4 0 3	2461.9965(2)	2462.03	2461.996 [125]	12 0 8	7024.091(1)	7024.10	7024.093 [142]	16 0 1	8714.1402(4)	8714.09	8714.139 [133]
4 0 4	2563.3403(2)	2563.32	2563.339 [125]	12 0 9	7029.844(1)	7030.51	7029.843 [142]	16 0 4	8877.042(1)	8877.02	8877.040 [142]
4 2 1	2333.64607(6)	2333.65	2333.646 [125]	12 0 10	7137.127(1)	7137.09	7137.127 [125]	16 0 7	8976.489(1)	8976.47	8976.488 [142]
4 2 2	2477.3089(2)	2477.33	2477.310 [125]	12 0 11	7194.365(1)	7194.95	7194.365 [134]	16 0 10	9108.322(3)	9108.34	9108.323 [150]
5 1 1	2799.1245(2)	2799.13	2799.124 [125]	12 0 12	7214.680(1)	7214.68	7214.680 [125]	16 0 11	9219.056(1)	9218.99	9219.056 [150]
5 1 2	2898.65323(6)	2898.65	2898.657 [125]	12 0 13	7340.792(1)	7341.29	7340.792 [134]	16 0 14	9294.994(1)	9294.98	9294.993 [150]
5 1 3	3047.0490(2)	3047.07	3047.048 [125]	12 0 14	7463.985(1)	7464.32	7463.986 [133]	16 0 15	9398.818(1)	9399.25	9398.817 [150]
5 1 4	3166.68(2)	3166.68	3166.685 [125]	12 0 15	7556.136(1)	7556.36	7556.135 [133]	16 0 17	9517.8741(8)	9518.10	9517.874 [150]
5 3 1	2919.0973(3)	2919.12	2919.098 [125]	12 0 16	7640.474(1)	7640.67	7640.476 [133]	16 0 18	9599.1039(8)	9601.02	9599.103 [174]
6 0 1	3363.9780(2)	3363.98	3363.978 [125]	12 2 1	6640.670(1)	6640.66	6640.667 [134]	16 0 19	9606.336(5)	9606.34	9606.332 [150]
6 0 2	3466.60018(6)	3466.62	3466.600 [125]	12 2 3	6782.826(2)	6782.81	6782.825 [134]	16 0 20	9690.0821(8)	9690.13	9690.082 [170]
6 0 3	3480.81930(6)	3480.82	3480.819 [125]	12 2 5	6894.268(2)	6894.22	6894.268 [158]	16 0 22	9874.2970(8)	9875.91	9874.296 [170]
6 0 4	3620.9430(2)	3620.92	3620.943 [125]	12 2 6	7039.494(2)	7039.73	7039.661 [142]	16 2 2	8749.056(1)	8749.07	8749.056 [133]
6 0 5	3748.2521(2)	3748.25	3748.252 [125]	12 2 7	7040.686(2)	7041.19	7040.685 [158]	16 2 4	8890.970(1)	8891.06	8890.970 [142]
6 0 6	3836.37100(3)	3836.35	3836.371 [125]	12 2 9	7207.024(1)	7207.62	7207.022 [134]	16 2 6	8980.053(1)	8979.95	8980.051 [175]
6 2 1	3375.6413(2)	3375.64	3375.642 [125]	12 2 10	7357.528(2)	7358.04	7357.528 [133]	16 2 7	9123.706(1)	9082.03	9123.706 [150]
6 2 2	3476.97731(6)	3477.01	3476.978 [125]	12 2 11	7491.112(2)	7491.48	7491.113 [133]	16 2 7	9123.706(1)	9123.85	9123.706 [150]
6 2 3	3634.1032(2)	3634.08	3634.104 [125]	12 2 12	7613.098(2)	7613.23	7613.098 [133]	16 2 11	9415.442(1)	9415.97	9415.442 [150]
6 2 4	3768.5551(2)	3768.55	3768.555 [125]	13 1 1	7127.796(1)	7127.77	7127.798 [125]	16 2 13	9545.384(1)	9545.79	9545.384 [170]
7 1 1	3932.0805(6)	3932.08	3932.083 [125]	13 1 7	7443.822(1)	7443.85	7443.746 [134]	16 2 16	9763.7896(8)	9765.71	9763.790 [174]
7 1 3	4062.8091(4)	4062.80	4062.809 [125]	13 1 8	7590.240(1)	7590.39	7590.244 [142]	17 1 1	9246.894(1)	9246.87	9246.893 [142]
7 3 1	3953.2921(2)	3953.29	3953.293 [125]	13 1 10	7715.885(2)	7715.96	7715.886 [134]	17 1 7	9538.070(5)	9538.21	9538.065 [142]
8 0 1	4417.37778(3)	4417.37	4417.378 [125]	13 1 12	7818.651(2)	7818.72	7818.650 [134]	17 1 14	9885.506(1)	9885.65	9885.509 [150]
8 0 4	4630.1613(2)	4630.14	4630.161 [125]	13 1 14	8047.173(1)	8047.85	8047.178 [134]	17 3 4	9445.920(1)	9446.11	9445.919 [142]
8 0 5	4730.82507(3)	4730.81	4730.825 [125]	13 1 15	8160.484(1)	8160.97	8160.484 [134]	17 3 14	9988.527(1)	9989.36	9988.522 [150]
8 0 8	5026.30302(3)	5026.27	5026.303 [125]	13 1 16	8267.106(1)	8268.17	8267.108 [133]	17 3 15	10112.1369(8)	10016.90	*10106.360* [170]
8 0 9	5105.67692(3)	5105.68	5105.677 [125]	13 3 7	7618.257(2)	7618.39	7618.257 [158]	18 0 1	9770.6360(8)	9770.61	9770.636 [170]
8 2 1	4502.1990(4)	4502.21	4502.199 [125]	14 0 1	7665.273(1)	7665.21	7665.273 [133]	18 0 7	10079.556(3)	10079.59	10079.565 [175]
9 1 1	4978.526(3)	4978.51	4978.524 [125]	14 0 3	7782.662(1)	7782.65	7782.662 [125]	18 0 8	10163.593(1)	10163.56	10163.598 [114]
9 1 4	5201.61(2)	5201.59	5201.613 [125]	14 0 5	7874.156(1)	7874.08	7874.156 [134]	18 0 12	10204.80(2)	10204.81	10204.806 [114]
9 1 5	5319.96(3)	5319.98	5320.001 [125]	14 0 8	7998.589(2)	7998.57	7998.585 [134]	18 0 13	10332.02(2)	10332.06	10332.013 [114]
9 1 8	5618.60187(3)	5618.60	5618.597 [125]	14 0 9	8083.953(1)	8083.91	8083.955 [134]	18 0 16	10429.15(2)	10428.98	10429.148 [114]
9 1 9	5723.651(1)	5723.66	5723.653 [125]	14 0 12	8276.326(1)	8276.44	8276.325 [142]	18 0 17	10504.41(3)	10504.45	10504.398 [114]
9 3 1	5074.0908(5)	5074.12	5074.091 [125]	14 0 14	8376.3502(8)	8376.32	8376.350 [142]	18 0 20	10640.61(2)	10641.28	10640.611 [114]
9 3 3	5227.459(1)	5227.44	5227.460 [125]	14 0 15	8452.6357(8)	8452.70	8452.636 [142]	18 2 1	9781.143(1)	9781.15	9781.143 [170]
10 0 3	5646.74022(3)	5646.73	5646.740 [125]	14 0 16	8475.7282(8)	8476.87	8475.724 [142]	19 1 10	10733.30(2)	10733.53	*10732.908* [114]
10 0 5	5762.372(1)	5762.31	5762.373 [125]	14 0 17	8612.948(1)	8613.96	8612.949 [142]	19 1 17	11000.56(2)	11000.67	*11000.160* [114]
10 0 7	5902.968(2)	5903.19	5902.966 [134]	14 0 18	8725.101(1)	8725.85	8725.100 [142]	19 3 1	10316.845(1)	10316.93	10316.848 [174]
10 0 8	5974.84501(3)	5974.81	5974.845 [125]	14 0 19	8810.765(1)	8811.42	8810.762 [142]	20 0 1	10815.251(5)	10815.24	10815.242 [170]
10 0 9	6058.668(2)	6058.81	6058.667 [125]	14 2 1	7676.0959(6)	7676.06	7676.095 [133]	20 0 2	10820.128(5)	10820.14	10820.142 [114]
10 0 10	6192.270(2)	6192.35	6192.271 [125]	14 2 4	7886.494(1)	7886.49	7886.494 [134]	20 0 11	11271.99(2)	11271.99	11271.988 [114]
10 0 12	6373.308(2)	6373.38	6373.308 [125]	14 2 7	8017.943(1)	8018.03	8017.945 [134]	21 1 1	11334.685(5)	11334.79	*11334.289* [111]
10 2 1	5540.9177(4)	5540.89	5540.917 [125]	14 2 10	8296.595(1)	8296.81	8296.594 [142]	22 0 4	11964.12(6)	11964.36	11964.252 [114]
10 2 4	5775.118(1)	5775.09	5775.118 [125]	14 2 12	8417.273(2)	8417.43	8417.273 [142]	22 0 5	12009.05(2)	12009.20	12009.029 [114]
11 1 1	6084.143(2)	6084.12	6084.143 [134]	14 2 13	8490.353(1)	8491.53	8490.353 [142]	24 0 2	12891.079(5)	12891.09	12891.153 [114]
11 1 3	6214.638(2)	6214.62	6214.640 [125]	14 2 14	8633.615(1)	8634.68	8633.614 [142]				
11 1 5	6327.090(1)	6327.02	6327.312 [142]	14 2 15	8762.569(1)	8763.39	8762.570 [142]				
11 1 6	6462.895(2)	6462.90	6462.898 [125]	15 1 1	8206.086(1)	8206.07	8206.090 [133]				
11 1 7	6470.361(1)	6470.80	6467.371 [158]	15 1 3	8336.6118(8)	8336.64	8336.611 [133]				

4.1. 04Toth [125]

The SISAM database contains 32 637 $^{14}N_2{}^{16}O$ rovibrational lines and covers the 525 – 7797 cm^{-1} wavenumber region. While most of these transitions were generated using effective Hamiltonians, the original measured values were retained for those transitions identified as being significantly perturbed by resonances. As a result, 1164 transitions from the SISAM data were identified as observed rather than calculated. Inspection showed that 43 of these transitions were provided by previous measurements by Toth [71,73,110]; thus, 1121 transitions were added to our compilation. An uncertainty of 0.000 5 cm^{-1} was used for these transitions, based on self-consistency with other transitions in our dataset.

We used the effective Hamiltonian parameters of 04Toth [125] to check our MARVEL energy levels. Results of this comparison can be seen in Fig. 3. Almost all of the differences are smaller than 0.01 cm^{-1}; the deviations are larger than 0.01 cm^{-1} only for relatively high J values ($J > 50$). We checked how many experimental measurements determine those MARVEL energy levels that have large difference from the 04Toth values and it turned out that most of them are determined by only one or two measurements (see the red squares in Fig. 3). While MARVEL levels determined by a single measurement must be regarded as less trustworthy, it is likely that the issue here is with poor extrapolation of the effective Hamiltonian used by 04Toth.

4.2. NOSL-296 [179]

The NOSL-296 line list [179] contains almost 900 000 lines, covering the 0.02 – 13 378 cm^{-1} wavenumber range. The authors published neither the values of the effective Hamiltonian parameters nor those of the energy levels; therefore, to make a meaningful comparison, we had to calculate them. Using the energy value of the lower quantum state of the transition, given in the line list, and values of the wavenumber entries, we could determine 67 028 rovibrational energy levels. During the comparison of these data with those of the present study, we identified an issue: there are significant differences between the measurements of 23KaMoTaCa [178] and the NOSL-296 [179] line positions. The Supplementary Material of 23KaMoTaCa [178] has indicated the presence of such differences. Therefore, we divided our comparison into two parts: (a) first we checked those MARVEL energy levels that are determined by at least three measured lines (see the

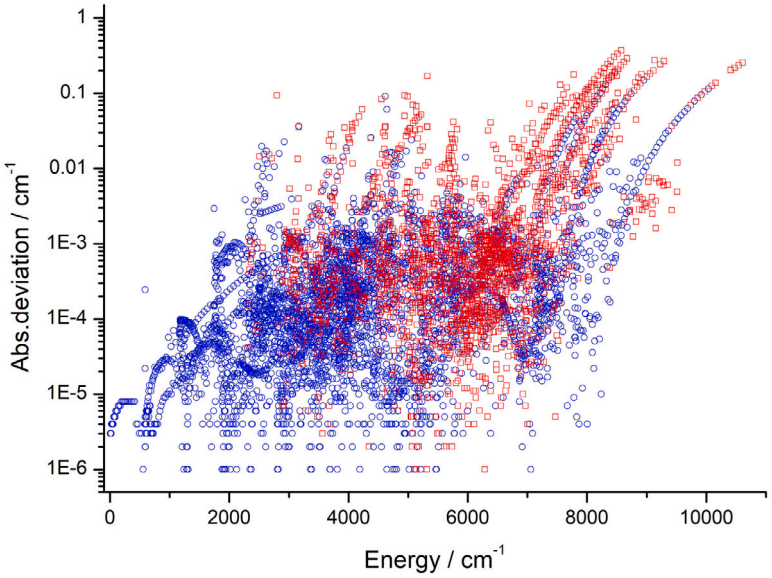

Fig. 3. Absolute deviations between the empirical (MARVEL) energy levels of this study and those of 04Toth [125]. Blue circles indicate states with MARVEL energies determined by at least three measured lines, while red squares correspond to the states with MARVEL energies determined by one or two measured lines.

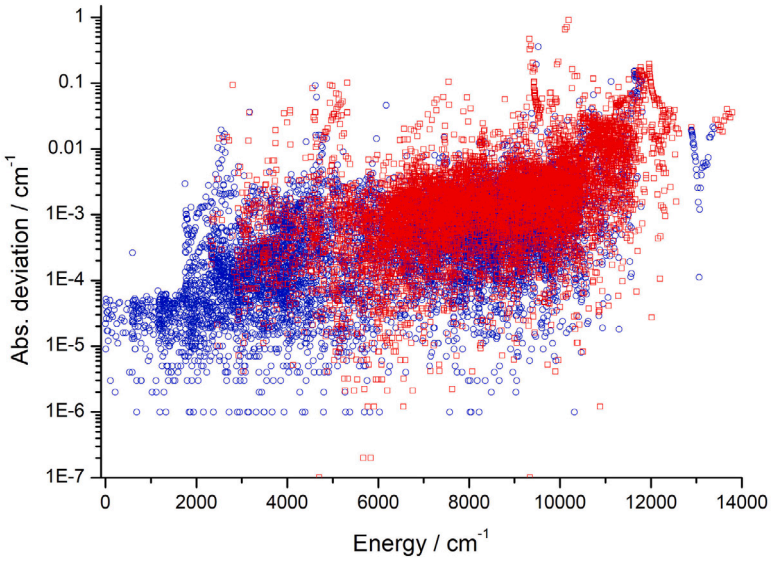

Fig. 4. Absolute deviations between the empirical (MARVEL) energy levels of this study and those of the NOSL-296 line list [179]; see text for the subset of NOSL-296 levels which could be utilized for this comparison. Blue circles indicate states with MARVEL energies determined by at least three measured lines, while the red squares correspond to the states with MARVEL energies determined by one or two measured lines.

blue circles in Fig. 4), in this case the average absolute difference is 0.001 5 cm^{-1}; (b) in the second step we compared those MARVEL levels with the NOSL-296 energies that are determined by one or two measured lines (see the red squares in Fig. 4). Although the average discrepancy is only 0.005 4 cm^{-1}, in this case we get several outliers, where the differences are larger that 0.01 cm^{-1}. Furthermore, we found 47 MARVEL energy levels which could not be found in the NOSL-296 energy level list within 1.0 cm^{-1}, most of these energy levels have a large polyad number ($P > 20$); these states are all present in both the Ames and our own variational line lists.

Using the first set of MARVEL energy list, we checked the NOSL-296 lines and collected those lines where the difference in the line positions is larger the 0.005 cm^{-1}. We found only 392 NOSL-296 lines that the MARVEL energies cannot reproduce within this limit. This list be can found in the Supplementary Material. These lines should be checked by the authors of NOSL-296.

5. Summary and conclusions

The present study has provided a comprehensive analysis of all the measured and assigned rovibrational lines of the parent isotopologue of nitrous oxide, $^{14}N_2{}^{16}O$. There are 91 sources considered in our final compilation, containing experimental wavenumbers with uncertainties and assignments. The experimental line data were analyzed and their assignments adjusted to a uniform set of polyads (P) and associated counting numbers (N). This canonical set of vibrational state assignments is recommended for future studies on the spectroscopy of nitrous oxide. The full list is given in the Supporting Material.

The corrected, self-consistent list of 67 930 rovibrational transitions contains 43 246 unique entries. This dataset underwent a Measured Active Rotational–Vibrational Energy Levels (MARVEL) analysis, yielding 17 561 empirical energy levels. These energy levels were validated using variational nuclear-motion calculations [177,201], the full details

of which will be published elsewhere [201]. Uncertainties for the empirical rovibrational energy levels were determined using a newly implemented bootstrap approach. We believe this approach yields more realistic uncertainties and, at least in part, compensates for both under- and overestimates of the published uncertainties of the transitions observed.

This study investigated more than 200 vibrational bands and yielded empirical energy values for 77 vibrational band origins (those with $\ell = 0$, where ℓ is the vibrational angular momentum quantum number). Our newly determined energy levels are being used to improve the $^{14}N_2{}^{16}O$ line list currently under construction both by providing energies to which an improved potential energy surface can be fit to and, in due course, which can be used to replace computed energies in the final line list.

Comparison with entries of the line lists SISAM [125] and NOSL-296 [179] revealed good overall agreement but also pointed out several minor issues with the data. Resolution of these problems requires future careful experimental and modeling studies.

CRediT authorship contribution statement

Jonathan Tennyson: Writing – original draft, Funding acquisition, Formal analysis, Conceptualization. **Tibor Furtenbacher:** Writing – original draft, Methodology, Formal analysis. **Sergei N. Yurchenko:** Formal analysis. **Attila G. Császár:** Writing – review & editing, Methodology.

Declaration of competing interest

The authors declare no competing financial interests.

Data availability

The data are included in the supplementary materials.

Acknowledgments

JT thanks the Distinguished Guest Scientists Fellowship Program-2022 of the Hungarian Academy of Sciences for funding his stays in Hungary and Zsolt Mezei for hosting him. We thank Oleg Polyansky for helpful discussions, Alain Campargue for supplying the transition line lists for 96Campargu [97] and 01CaWeTaPe [114], and Xinchuan Huang for making the Ames line list available prior to publication. This work was supported by the European Research Council (ERC) under the European Union's Horizon 2020 research and innovation program through Advanced Grant number 883830. The work performed in Budapest received support from the HUN-REN Hungarian Research Network and the National Research, Development, and Innovation Office (NKFIH, grant no. K138233). This paper supports work within the COST (European Cooperation in Science and Technology) action CA21101 "Confined molecular systems: from a new generation of materials to the stars (COSY)".

Appendix A. Notes on data sources

Some sources, notably **60TiPlBe** [17], **70PeSuFr** [30], **74FaDu** [44], and **18LaScAgMe** [157], used the (c,d) notation instead of the (e,f) one [209]. We assumed that c corresponds to e and d to f. All other comments are listed source by source.

50HeHe [7]: This older source was the first detailed study of the near-infrared transitions in N_2O. By modern standards, it is relatively inaccurate, claiming a precision of 0.03 cm^{-1} for unblended lines. The source gives a calibration uncertainty of 0.08 cm^{-1}. However, there appears to be no subsequent high resolution measurements of the $(P\ell N) = (22\,0\,4)$ band centered at 11 964.3 cm^{-1}. Recalibration of this source by a factor of 0.999 998 11 corresponds to a shift of −0.02 cm^{-1}. Therefore, we adopted an uncertainty of 0.03 cm^{-1}, which was doubled for lines marked as blended with either other N_2O transitions or water lines.

60TiPlBe [17]: This source presents measurements of 2522 lines for a large number of vibrational bands. However, for most bands the values given are calculated with an unsigned obs−calc, meaning that it is not possible to reliably recover the experimental wavenumbers. Only 884 lines (for which there is no effective Hamiltonian fit given) were retained as these correspond to the actual measured wavenumbers: these lines are in any case for the more interesting (*i.e.*, less studied) bands. The paper implies an uncertainty of 0.002 cm^{-1} but the lines retained are only given to two decimal digits; thus, these uncertainties were increased.

64LaLi [22]: No 'e'/'f' designation was given for transitions within the 02^20 $[(P\ell N) = (2\,2\,1)]$ state; thus, these transitions were assumed to be degenerate and each line was included twice in our MARVEL database.

71LeHoThMa [33]: This source gives five transitions corresponding to $J = 3 - 2$ transitions in low-lying vibrational bands. As no uncertainties were given, 100 kHz was assumed by us. One of these measurements was not consistent with subsequent studies and had to be removed.

74FaDu [44]: Provides an unusual early fluorescence spectrum. The tables which were scanned are of poor quality, which gives some uncertainty over precise values for some of the lines.

74KrSa [46]: The authors did not specify uncertainties; thus, 0.02 cm^{-1} was assumed, with 0.04 cm^{-1} for blended lines, based on the use of combination differences. Transitions involving degenerate bands did not give 'e'/'f' parities; thus, they were included twice.

74BuVaGeKa [43]: The uncertainties attached to the transitions of this source were doubled, as suggested in 78Lovas [210].

75Bogey [49]: This source gives pure rotational transitions within the $(P\ell N) = (4\,0\,1)$ vibrational state. As suggested by 14TiChChCh [146], the uncertainties of this source should be increased as there are calibration issues with the data. The uncertainties were increased by a factor of three compared to the original values quoted in the paper.

75WhSuRiHa [54]: An uncertainty of 25 kHz was assumed.

76AmGu [55]: This publication is an early example of a high-accuracy infrared spectrum (with an uncertainty of 0.000 2 cm^{-1}). The transitions are given as a comprehensive table in the paper but, unfortunately, with poor print quality. The results were extensively cleaned but even then there were many cases where the transition wavenumber could not be read with certainty. These cases were marked as not validated. The (7 3 1) – (3 3 1) band was not given a parity, so it was assumed to represent both parities and duplicated. Transitions in the region where the (6 0 2) and (6 0 3) states interact were not consistent with those measured subsequently; therefore, they were removed from the analysis. Calibration tests suggested that the calibration of the spectrum was in line with more modern sources.

76AnBuKaKr [56]: This source contains a number of high-resolution pure rotational transitions. The fine structure (e/f) splitting within the (3 3 1) state was not resolved, each line is given twice, and the uncertainties were increased to 35 kHz.

78ReMeDy [58]: This paper presents hyperfine-resolved rotational transitions. A simple average was performed over the hyperfine components and the uncertainty was set to 150 Hz.

82Guelachv [63]: The wavenumbers of this study were scaled by a calibration factor of 0.999 999 890, which is in line with later suggestions that the spectrum needs recalibration by about 15 MHz.

84Toth [67]: A wavenumber uncertainty of 0.000 2 cm^{-1} was chosen based on combination differences.

87HiWeMa [72]: The fine structure (e/f) splitting within the (3 3 1) state was not resolved; thus, each line is given twice and the uncertainties were increased to 35 kHz.

95CaPeBaTe [93]: The wavenumbers were scaled by a calibration factor of 1.000 003 08.

96TaEvZiMa [100]: As suggested by 14TiChChCh [146], the uncertainties were increased by a factor of 1.6. The v_1 and v_3 vibrational state labels were swapped.

96MaRaHeVa [99]: The authors studied pressure shifts for two lines in the v_3 or (2 0 2) band. However, the stated zero pressure line positions do not agree well with other measurements; thus, these lines were not validated.

96WeSiRe [101]: An uncertainty of 0.000 6 cm^{-1} was assumed.

98GaCaKaSt [105]: The authors declare an uncertainty of 0.005 cm^{-1}; this was doubled to 0.01 cm^{-1} for lines blended with water lines. It was necessary to reassign the P branch lines.

99Toth [110]: This paper reports a number of resonance interactions. Those involving the (8 0 3) and (8 0 4) bands do not give consistent combination differences and the associated transitions were removed. For other resonance pairs the uncertainties were increased.

00WeKaCaBa [111]: This source reports both ICLAS and FTS transition wavenumbers. For the ICLAS data an uncertainty of 0.005 cm^{-1} is given; lines marked as blended or weak were given an uncertainty of 0.01 cm^{-1}. For the FTS data, 0.000 5 cm^{-1} was used below 6300 cm^{-1}, which was linearly increased to 0.005 5 cm^{-1} at 11 300 cm^{-1} as suggested in the paper. The J's in the (18 0 3) – (0 0 1) band's R branch transitions were renumbered. Resonance lines in the (13 1 7) – (1 1 1) hot band were assigned to (13 1 6) – (1 1 1). The P(12) line in the (20 0 2) – (0 0 1) band (line 00WeKaCaBa.12) was changed from 10 818.209 0 to 10 808.209 0. Extra resonance lines P(32) (06WaPeTaGa.2327) and P(33) (06WaPeTaGa.2328) in the band (16 0 7) – (0 0 1) were assigned to (16 0 6) – (0 0 1).

01BaVe [113]: Bands for which the e/f splitting was unresolved were duplicated. An uncertainty of 0.008 cm^{-1} (given as the upper limit in the paper) was adopted.

01CaWeTaPe [114]: An uncertainty of 0.015 cm^{-1} was assumed, except for lines designated as lines overlapping with atmospheric water lines, lines overlapping with other N_2O lines, or very weak lines, for which an uncertainty of 0.030 cm^{-1} was adopted.

03BaPiVe [118]: This source gives three bands with unresolved e/f splitting, each were included in our analysis twice. Uncertainty estimated as 0.000 4 cm^{-1}, based on data in the paper.

03DiPeTaTe [119]: An uncertainty of 0.003 cm^{-1} was adopted from the paper, except for blended or degenerate lines, for which an uncertainty of 0.006 cm^{-1} was used. For band (16 0 17) – (0 0 1), the lines R(32) – R(36) were removed, as they have been reasigned by 04BeCaPeTa.

04BeCaPeTa [123]: An uncertainty of 0.005 cm^{-1} was taken from the paper; for lines marked as blended with water lines this uncertainty was doubled. The paper includes correction of a few misprints in the rovibrational parameters and the reconsideration of the analysis of an inter-polyad Coriolis interaction system given in 03DiPeTaTe [119]. Resonance lines in (16 0 17) – (0 0 1) were re-assigned to the e branch of (17 1 6) – (0 0 1). Three lines overlapping with water lines were removed as they were inconsistent with other sources.

04NeSuVa [124]: An uncertainty of 0.000 5 cm^{-1} was adopted from the paper.

04Toth [125]: This source is discussed in Section 4.1.

06HePiGuSo [128]: Q branches (both e – f and f – e) in the (9 1 9) – (3 1 1) band were removed as they are inconsistent with other transitions given in this source and elsewhere, such as 19BeMoKaKa [158]. Eleven lines were removed as they involve J values lower than the ℓ value of the given vibrational state, which is unphysical. The six highest P(J) lines from the (10 2 4)e – (3 1 1)e band were removed as they disagree with other sources, notably 19BeMoKaKa [158], where the assignments are confirmed by combination differences. The (2 2 1)f band was removed as it was assigned using an incorrect value for the D centrifugal distortion constant, taken from Toth [125], and therefore gave wavenumbers which disagree with other sources. This source also includes corrections of a few misprints in the rovibrational parameters and the reconsideration of the analysis of an interpolyad Coriolis interaction system given in 03DiPeTaTe [119].

06WaPeTaGa [129]: An uncertainty of 0.005 cm^{-1} was adopted from the paper, except for lines blended with water lines, for which an uncertainty of 0.01 cm^{-1} was assumed. The band (14 0 8) – (0 0 1) centered at 7998.59 cm^{-1} has extra lines for J = 28 and 29, presumably due to resonances. The interacting state is unassigned so the extra lines were removed. The R(28) and R(29) lines in the (11,1,11) f – (1,1,1) f band were reassigned to R(29) and R(30), respectively. This source contains 908 lines which are exactly the same as in 00WeKaCaBa [111]. Since lists of co-authors of these two publications contain no overlaps, both sets of lines were kept.

07Horneman [132]: Following 14TiChChCh [146], all transitions in the (1 1 1) – (0 0 1) band were retained, even those with zero weights in the fit. Nevertheless, 24 lines had to be removed, on the basis of inconsistency with other sources, including transitions in the (2 0 0) – (1 1 1) and (2 2 1) – (1 1 1) bands, which were zero-weighted in the original paper. 14TiChChCh [146] states it is necessary to remove 38 lines from 07Horneman but does not specify which.

07LiKaMaRo [133]: Q branches for bands with $\ell > 0$ for both upper and lower states have the wrong selection rules (e – e or f – f). We assumed that the parity of the lower state is given correctly on the basis of consistency with other sources. On this basis the following corrections were made (in the harmonic oscillator notation used in the original source): 52^20f – 02^20f to 52^20e – 02^20f; 35^10e – 01^10e to 35^10f – 01^10e; 35^10f – 01^10f to 35^10e – 01^10f; 02^23e – 02^20e to 02^23f – 02^20e; 02^23f – 02^20f to 02^23e – 02^20f; 51^10e – 01^10e to 51^10f – 01^10e; 51^10f – 01^10f to 51^10e – 01^10f. The 36^20 – 02^20 band does not have the ℓ-doubling resolved; thus, it was given twice with the correct selection rules. Lines P(19)–P(36) in the 32^01e – 02^00e band were reassigned to P(18)–P(35); lines P(16)–P(18) in the 36^20e – 02^20e band were reassigned to P(15)–P(17). Line Q(22) in the 35^01f – 01^10f band was reassigned to Q(23). Lines Q(16)–Q(18) in the 51^10e – 01^10f band were reassigned to Q(17)–Q(19). Finally, the Q(10) line at 6302.655 1 cm^{-1} in the (11 1 11)e – (1 1 1)f band was reassigned to the (12 2 12)e – (1 1 1)f band. This source contains 90 lines which appear to be duplicates of lines in 99Toth [110]. These duplicate lines were kept during the MARVEL analysis. Furthermore, this source contains 47 lines which also appear in 09LiKaPeHu [136]. These duplicate lines were kept only here.

07LiKaPeTa [134]: The band centered at about 6770 cm^{-1} given as 0*10e – 0000e is assumed to be 0(11)0e – 0000e, which is (11 1 10)e – (0 0 1)e in polyad notation. In the R branch of the (10 0 9)e – (0 0 1)e band lines R(51)–R(55) were reassigned to R(50)–R(54). This source contains 172 lines which also appear in the source 09LiKaPeHu [136]. The identical lines were only kept here.

09LiKaPeHu [136]: Both the e and f components of the (14 2 15) – (2 2 1) band contained an unresolved P(2) line at 6836.036 5 cm^{-1}, which are unphysical and thus were removed. Line R(58) in the (13 1 7)e – (1 1 1)e band was reassigned to R(57). Line R(42) in the (14 2 5)e – (2 2 1)e band was reassigned as R(42)f. This source contains 55 lines which also appear in the source 12LuMoLiPe [142]. These identical lines were only kept here.

11LiKaPeTa [140]: This source contains 391 lines which also appear in the source 12LuMoLiPe [142]. These lines were deleted in the list of lines of 12LuMoLiPe.

12LuMoLiPe [142]: Line 12LuMoLiPe.3047, assigned as P(1) (13 1 4) e – (0 0 1)e, was removed as being unphysical.

16KaCaKaPe [150]: The R(39) line at 7989.890 25 cm^{-1}, assigned as 35^11f – 01^10f in the original paper, was reassigned to 31^11f – 01^10f or (15 1 8)f, in line with its neighboring transitions. Four lines reassigned and given by 22KaTaKaCab [175] were removed. 526 lines recorded by 16KaCaKaPe but assigned by 22KaTaKaCab were added. Lines 16KaCaKaPe.3134 and 16KaCaKaPe.3135 denoted as "extra lines" by 22KaTaKaCab were assigned to the band (15 1 7)e – (1 1 1)e. This source contains 171 duplicate transitions, we kept one of the duplicate entries.

19BeMoKaKa [158]: Assignments of the (10 0 5) e and (10 0 6) e bands were swapped.

20ZhBaFlHo [164]: The stated frequencies were doubled to allow for two-photon transitions; the corresponding uncertainties were also doubled.

21KaKaTaCa [170]: No uncertainty is stated; a value of 0.001 cm^{-1} was assumed.

22KaTaKaCaa [174] Nine lines in the range 22KaTaKaCaa.2461 to 22KaTaKaCa.2505 were reassigned to (16 0 19)e instead of (16 0 17). The P(36) line at 8556.241 90 cm^{-1} was reassigned from (18 0 4)e – (2 0 2)e to (17 1 1)e – (2 0 2)e. This source contains two duplicated transitions, we deleted one of the duplicated entries.

22KaTaKaCab [175]: Ten lines identified as in resonance with (15 1 8) assigned to (15 1 7); six lines identified as in resonance with (16 0 10) assigned to (16 2 16). 526 lines measured by 16KaCaKaPe [150] were assigned; these are the last lines labeled as 16KaCaKaPe. Resonances lines in the (16 2 7) – (2 2 1) band involving $J' = 35$ and 36 were reassigned to (15 1 13) – (2 2 1), as suggested in the paper. This source contains 28 duplicated transitions, we had to delete one duplicate entry.

22LuGo [176]: An uncertainty of 0.01 cm^{-1} was assumed, except for lines marked as blended, for which 0.02 cm^{-1} was used.

24SiSeEmMa [180]: After the original submission of our paper, this new source became available and was added as part of the revision process. Bands (18 0 4), (18 0 8) and (18 0 9) were relabeled (18 0 3), (18 0 7) and (18 0 8), respectively, in line with our proposed canonical numbering scheme. Four lines which do not obey combination differences, even within the 24SiSeEmMa dataset, were removed.

Appendix B. Supplementary material

See supplementary material for the MARVEL input (transitions) file and output (energy) file. A comprehensive table of vibrational levels with associated polyad quantum number is also given.

Supplementary material associated with this article can be found, in the online version, at https://doi.org/10.1016/j.jqsrt.2024.108902.

References

[1] Ravishankara AR, Daniel JS, Portmann RW. Nitrous oxide (N_2O): The dominant ozone-depleting substance emitted in the 21st century. Science 2009;326(5949):123–5. http://dx.doi.org/10.1126/science.1176985.

[2] Vasquez M, Schreier F, Garcia SG, Kitzmann D, Patzer B, Rauer H, et al. Infrared radiative transfer in atmospheres of earth-like planets around F, G, K, and M stars. Clear-sky thermal emission spectra and weighting functions. Astron Astrophys 2013;549:A26. http://dx.doi.org/10.1051/0004-6361/201219898.

[3] Grenfell JL. A review of exoplanetary biosignatures. Phys Rep 2017;713:1–17. http://dx.doi.org/10.1016/j.physrep.2017.08.003.

[4] Tinetti G, Beaulieu J, Henning T, Meyer M, Micela G, Ribas I, et al. EChO. Exp Astron 2012;34:311–53.

[5] Tinetti G, Drossart P, Eccleston P, Hartogh P, Heske A, Leconte J, et al. A chemical survey of exoplanets with ARIEL. Exp Astron 2018;46:135–209. http://dx.doi.org/10.1007/s10686-018-9598-x.

[6] Coles DK, Elyash ES, Gorman JG. Microwave absorption spectra of N_2O. Phys Rev 1947;72:973. http://dx.doi.org/10.1103/PhysRev.72.973.2.

[7] Herzberg G, Herzberg L. Rotation-vibration spectra of diatomic and simple polyatomic molecules with long absorbing paths. 6. The spectrum of nitrous oxide (N_2O) below 1.2 μm. J Chem Phys 1950;18:1551–61. http://dx.doi.org/10.1063/1.1747539.

[8] Callomon HJ, McKean DC, Thompson HW. Intensities of vibration bands. 3. Nitrous oxide. Proc R Soc London Ser A 1951;208:332–41. http://dx.doi.org/10.1098/rspa.1951.0164.

[9] Johnson CM, Trambarulo R, Gordy W. Microwave spectroscopy in the region from two to three millimeters, Part II. Phys Rev 1951;84:1178–80. http://dx.doi.org/10.1103/PhysRev.84.1178.

[10] Tetenbaum SJ. 6-millimeter spectra of OCS and N_2O. Phys Rev 1952;88:772–4. http://dx.doi.org/10.1103/PhysRev.88.772.

[11] Douglas AE, Moller CK. The near infrared spectrum and the internuclear distances of nitrous oxide. J Chem Phys 1954;22:275–9. http://dx.doi.org/10.1063/1.1740051.

[12] Burrus CA, Gordy W. Millimeter and submillimeter wave spectroscopy. Phys Rev 1956;101:599–602. http://dx.doi.org/10.1103/PhysRev.101.599.

[13] Lakshmi K, Rao KN, Nielsen HH. Molecular constants of nitrous oxide from measurements of ν_2 at 17 μm. J Chem Phys 1956;24:811–3. http://dx.doi.org/10.1063/1.1742614.

[14] Plyler EK, Tidwell ED, Allen HC. Near infrared spectrum of nitrous oxide. J Chem Phys 1956;24:95–7. http://dx.doi.org/10.1063/1.1700878.

[15] Shearer JN, Wiggins TA, Guenther AH, Rank DH. L-type doubling in N_2O. J Chem Phys 1956;25:724–9. http://dx.doi.org/10.1063/1.1743037.

[16] Clough SA, McCarthy DE, Howard JN. $4\nu_2$ band of nitrous oxide. J Chem Phys 1959;30:1359–61. http://dx.doi.org/10.1063/1.1730192.

[17] Tidwell ED, Plyler EK, Benedict WS. Vibration–rotation bands of N_2O. J Opt Soc Amer 1960;50:1243–63. http://dx.doi.org/10.1364/JOSA.50.001243.

[18] Rank DH, Wiggins TA, Rao BS, Eastman DP. Highly precise wavelengths in infrared. 2. HCN, N_2O, and CO. J Opt Soc Am 1961;51:929. http://dx.doi.org/10.1364/JOSA.51.000929.

[19] Burch DE, Williams D. Total absorptance by nitrous oxide bands in the infrared. Appl Opt 1962;1:473–82. http://dx.doi.org/10.1364/AO.1.000473.

[20] Rao KN, de Vore RV, Plyler EK. Wavelength calibrations in the far infrared (30 to 1000 microns). J Res Natl Inst Stand Technol 1963;67A:351–8. http://dx.doi.org/10.6028/jres.067A.038.

[21] Gordon HR, McCubbin TK. 0220-0110 band of $^{14}N_2{}^{16}O$. J Opt Soc Amer 1964;54:956. http://dx.doi.org/10.1364/JOSA.54.000956.

[22] Lafferty WJ, Lide DR and. Rotational constants of excited vibrational states of $^{14}N_2$ ^{16}O. J Mol Spectrosc 1964;14:407. http://dx.doi.org/10.1016/0022-2852(64)90134-1.

[23] Pliva J. Infrared spectra of isotopic nitrous oxides. J Mol Spectrosc 1964;12:360. http://dx.doi.org/10.1016/0022-2852(64)90020-7.

[24] Plyler EK, Tidwell ED, Maki AG. Infrared absorption spectrum of nitrous oxide (N_2O) from 1830 cm^{-1} to 2270 cm^{-1}. J Res Natl Inst Stand Technol 1964;68A:79–86. http://dx.doi.org/10.6028/jres.068A.006.

[25] Harmony MD, Sancho M.^{14}N quadrupole coupling constants in N_2O by high-resolution microwave spectroscopy. J Chem Phys 1966;45:1812–5. http://dx.doi.org/10.1063/1.1727836.

[26] Berendts BT, Dymanus A. Evaluation of molecular quadrupole moments from broadening of microwave spectral lines. I. Measurements. J Chem Phys 1968;48:1361–7. http://dx.doi.org/10.1063/1.1668803.

[27] French IP, Arnold TE. Foreign-gas broadening of $J = 5 - 6$ rotational transition of nitrous oxide. J Mol Spectrosc 1968;27:218–24. http://dx.doi.org/10.1016/0022-2852(68)90031-3.

[28] Pliva J. Some near infrared bands of nitrous oxide. J Mol Spectrosc 1968;25:62–76. http://dx.doi.org/10.1016/S0022-2852(68)80031-1.

[29] Pliva J. Molecular constants of nitrous oxide $^{14}N_2{}^{16}O$. J Mol Spectrosc 1968;27:461–88. http://dx.doi.org/10.1016/0022-2852(68)90053-2.

[30] Pearson R, Sullivan T, Frenkel L. Microwave spectrum and molecular parameters for $^{14}N_2{}^{16}O$. J Mol Spectrosc 1970;34:440–9. http://dx.doi.org/10.1016/0022-2852(70)90025-1.

[31] Pliva J. Photographic infrared bands $5\nu_3$ and $4\nu_2^0 + 4\nu_3$ of $^{14}N_2{}^{16}O$. J Mol Spectrosc 1970;33:500–4. http://dx.doi.org/10.1016/0022-2852(70)90143-8.

[32] Scharpen LH, Muenter JS, Laurie VW. Electric polarizability anisotropies of nitrous oxide, propyne, and carbonyl sulfide by microwave spectroscopy. J Chem Phys 1970;53:2513–9. http://dx.doi.org/10.1063/1.1674355.

[33] Lemaire J, Houriez J, Thibault J, Maillard B. Infrared microwave double resonance in methyl bromide and nitrous oxide. J Phys 1971;32:35. http://dx.doi.org/10.1051/jphys:0197100320103500, – &.

[34] Toth RA. Line strengths of N_2O in 2.9 μm region. J Mol Spectrosc 1971;40:588–604. http://dx.doi.org/10.1016/0022-2852(71)90260-8.

[35] Toth RA. Self-broadened and N_2 broadened linewidths of N_2O. J Mol Spectrosc 1971;40:605–15. http://dx.doi.org/10.1016/0022-2852(71)90261-X.

[36] Lowder JE. Band intensity and line half-width measurements in N_2O near 4.5 μm. J Quant Spectrosc Radiat Transff 1972;12:873–80. http://dx.doi.org/10.1016/0022-4073(72)90075-1.

[37] Margolis JS. Intensity and half-width measurements of $(00^02 - 00^00)$ band of N_2O. J Quant Spectrosc Radiat Transfer 1972;12:751–7. http://dx.doi.org/10.1016/0022-4073(72)90180-X.

[38] Sokoloff DR, Javan A. Precision spectroscopy of N_2O, $(00^01) - (10^00)$ laser band by frequency mixing in an infrared, metal–metal oxide-metal point contact diode. J Chem Phys 1972;56:4028–31. http://dx.doi.org/10.1063/1.1677811.

[39] Tien CL, McCreigh CR, Modest MF. Infrared radiation properties of nitrous-oxide. J Quant Spectrosc Radiat Transfer 1972;12:267–77. http://dx.doi.org/10.1016/0022-4073(72)90037-4.

[40] Lacome N, Boulet C, Arie E. Spectroscopy using laser source. 3. Intensities and lengths of transition lines of nitrogen protoxide - deviation of Lorentz line shape. Can J Phys 1973;51:302–10. http://dx.doi.org/10.1139/p73-038.

[41] Tubbs LD, Williams D. Broadening of infrared-absorption lines at reduced temperatures. 3. Nitrous-oxide. J Opt Soc Am 1973;63:859–63. http://dx.doi.org/10.1364/JOSA.63.000859.

[42] Amiot C, Guelachvili G. Vibration–rotation bands of $^{14}N_2{}^{16}O$ - 1.2 – 3.3 μm region. J Mol Spectrosc 1974;51:475–91. http://dx.doi.org/10.1016/0022-2852(74)90202-1.

[43] Burenin AV, Valbov AN, Gershtein LI, Karyakin EN, Krupnov AF, Maslovskii AV, et al. Submillimeter spectrum and intermolecular parameters. Opt Spectrosc 1974;37:676.

[44] Farrenq R, Dupre-Maquaire J. Vibrational luminescence of N_2O excited by DC discharge - rotation-vibration constants. J Mol Spectrosc 1974;49:268–79. http://dx.doi.org/10.1016/0022-2852(74)90275-6.

[45] Farrenq R, Gaultier D, Rossetti C. Vibrational luminescence of N_2O excited by DC discharge - Emission-lines intensities and populations of rotational-vibrational levels. J Mol Spectrosc 1974;49:280–8. http://dx.doi.org/10.1016/0022-2852(74)90276-8.

[46] Krell JM, Sams RL. Vibration–rotation bands of nitrous-oxide - 4.1 μm region. J Mol Spectrosc 1974;51:492–507. http://dx.doi.org/10.1016/0022-2852(74)90203-3.

[47] Varanasi P, Bangaru BRP. Measurement of line-intensities of linear molecules under low resolution. J Quant Spectrosc Radiat Transf 1974;14:1253–7. http://dx.doi.org/10.1016/0022-4073(74)90093-4.

[48] Blanquet G, Walrand J, Courtoy CP. Vibration–rotation bands of isotopic-species of N_2O in 4.5 μm region. Ann de la Soc Sci de Bruxelles Ser 1-Sci Math Astron Et Phys 1975;89:93–114.

[49] Bogey M. Microwave-absorption spectroscopy in ν_3 states of OCS and N_2O through energy-transfer from N_2^*. J Phys B: At Mol Opt Phys 1975;8:1934–8. http://dx.doi.org/10.1088/0022-3700/8/11/028.

[50] Boissy JP, Valentin A, Cardinet P, Claude ML, Henry A. Line intensities of the ν_3 fundamental band of nitrous oxide. J Mol Spectrosc 1975;57:391–6. http://dx.doi.org/10.1016/0022-2852(75)90299-4.

[51] Casleton KH, Kukolich SG. Beam maser measurements of hyperfine-structure in $^{14}N_2O$. J Chem Phys 1975;62:2696–9. http://dx.doi.org/10.1063/1.430854.

[52] Dupre-Maquaire I, Pinson P. Emission spectrum of N_2O in 8 μm range. J Mol Spectrosc 1975;58:239–49.

[53] Toth RA, Farmer CB. Line strengths of H_2O and N_2O in 1900 cm^{-1} region. J Mol Spectrosc 1975;55:182–91. http://dx.doi.org/10.1016/0022-2852(75)90263-5.

[54] Whitford BG, Siemsen KJ, Riccius HD, Hanes GR. Absolute frequency measurements of N_2O laser transitions. Opt Commun 1975;14:70–4. http://dx.doi.org/10.1016/0030-4018(75)90060-7.

[55] Amiot C, Guelachvili G. Extension of 106 samples Fourier spectrometry to indium-antimonide region - Vibration-rotation bands of $^{14}N_2{}^{16}O$ 3.3-5.5 μm region. J Mol Spectrosc 1976;59:171–90. http://dx.doi.org/10.1016/0022-2852(76)90289-7.

[56] Andreev BA, Burenin AV, Karyakin EN, Krupnov AF, Shapin SM. Submillimeter wave spectrum and molecular-constants of N_2O. J Mol Spectrosc 1976;62:125–48. http://dx.doi.org/10.1016/0022-2852(76)90344-1.

[57] Valentin A, Lemoal MF, Cardinet P, Boissy JP. High precision spectrum of N_2O at 4.5 μm and determination of molecular constants for ν_3 and $(\nu_2+\nu_3-\nu_2)$ bands. J Mol Spectrosc 1976;59:96–102. http://dx.doi.org/10.1016/0022-2852(76)90045-X.

[58] Reinartz JMLJ, Meerts WL, Dymanus A. Hyperfine-structure, electric and magnetic-properties of $^{14}N_2{}^{16}O$ in ground and 1st excited bending vibrational state. Chem Phys 1978;31:19–29. http://dx.doi.org/10.1016/0301-0104(78)87022-0.

[59] Braund DB, Cole ARH, Cugley JA, Honey FR, Pulfrey RE, Reece GD. Precise measurements with a compact vacuum infrared spectrometer. Appl Opt 1980;19:2146–52. http://dx.doi.org/10.1364/AO.19.002146.

[60] Nagai K, Kawaguchi K, Yamada C, Hayakawa K, Takagi Y, Hirota E. A high-precision wavelength meter for tunable diode laser: Measurements of CO_2 and N_2O bands at 10 μm. J Mol Spectrosc 1980;84:197–203. http://dx.doi.org/10.1016/0022-2852(80)90253-2.

[61] Lacome N, Levy A. Line strengths and self-broadened linewidths of N_2O in the 2-μm region: 2400 – 0000 and 0112 – 0000 transitions. J Mol Spectrosc 1981;85:205–14. http://dx.doi.org/10.1016/0022-2852(81)90319-2.

[62] Olson WB, Maki AG, Lafferty WJ. Tables of N_2O absorption-lines for the calibration of tunable infrared-lasers from 522 cm^{-1} to 657 cm^{-1} and from 1115 cm^{-1} to 1340 cm^{-1}. J Phys Chem Ref Data 1981;10:1065–84. http://dx.doi.org/10.1063/1.555651.

[63] Guelachvili G. Absolute N_2O wavenumbers between 1118 and 1343 cm^{-1} by Fourier-transform spectroscopy. Can J Phys 1982;60:1334–47. http://dx.doi.org/10.1139/p82-181.

[64] Jolma K, Kauppinen J, Horneman VM. Vibration–rotation spectrum of N_2O in the region of the lowest fundamental ν_2. J Mol Spectrosc 1983;101:278–84. http://dx.doi.org/10.1016/0022-2852(83)90133-9.

[65] Lacome N, Levy A, Guelachvili G. Fourier-transform measurement of self-broadening, N_2-broadening, and O_2-broadening of N_2O lines - Temperature-dependence of linewidths. Appl. Optics 1984;23:425–35. http://dx.doi.org/10.1364/AO.23.000425.

[66] Pollock CR, Petersen FR, Jennings DA, Wells JS, Maki AG. Absolute frequency measurements of the 00(0)2-00(0)0, 20(0)1-00(0)0, and 12(0)1-00(0)0 bands of N_2O by heterodyne spectroscopy. J Mol Spectrosc 1984;107:62–71. http://dx.doi.org/10.1016/0022-2852(84)90265-0.

[67] Toth RA. Line strengths of N_2O in the 1120-1440-cm^{-1} region. Appl Opt 1984;23:1825–34. http://dx.doi.org/10.1364/AO.23.001825.

[68] Brown LR, Toth RA. Comparison of the frequencies of NH_3, CO_2, H_2O, N_2O, CO, and CH_4 as infrared calibration standards. J Opt Soc Am B 1985;2:842–56. http://dx.doi.org/10.1364/JOSAB.2.000842.

[69] Wells JS, Hinz A, Maki AG. Heterodyne frequency measurements on N_2O between 1257 and 1340 cm^{-1}. J Mol Spectrosc 1985;114:84–96. http://dx.doi.org/10.1016/0022-2852(85)90339-X.

[70] Wells JS, Jennings DA, Hinz A, Murray JS, Maki AG. Heterodyne frequency measurements on N_2O at 5.3 and 9.0 μm. J Opt Soc Amer B 1985;2:857–61. http://dx.doi.org/10.1364/JOSAB.2.000857.

[71] Toth RA. Frequencies of N_2O in the 1100 cm^{-1} to 1440 cm^{-1} region. J Opt Soc Amer B 1986;3:1263–81. http://dx.doi.org/10.1364/JOSAB.3.001263.

[72] Hinz A, Wells JS, Maki AG. Heterodyne measurements of hot bands and isotopic transitions of N_2O near 7.8 μm. Z Phys D 1987;5:351–8. http://dx.doi.org/10.1007/BF01385466.

[73] Toth RA. N_2O vibration–rotation parameters derived from measurements in the 900−1090-cm^{-1} and 1580−2380-cm^{-1} regions. J Opt Soc Amer B 1987;4:357–74. http://dx.doi.org/10.1364/JOSAB.4.000357.

[74] Zink LR, Wells JS, Maki AG. Heterodyne frequency measurements on N_2O near 1060 cm^{-1}. J Mol Spectrosc 1987;123:426–33. http://dx.doi.org/10.1016/0022-2852(87)90289.

[75] Esplin MP, Barowy WM, Huppi RJ, Vanasse GA. High resolution Fourier spectroscopy of nitrous oxide at elevated temperatures. Mikrochim Acta 1988;2:403–7.

[76] Amrein A, Hollenstein H, Quack M, Schmitt U. High resolution interferometric Fourier transform infrared spectroscopy in supersonic free jet expansions: N_2O, $CBrF_3$ and CF_3I. Infrared Phys 1989;29:561–74. http://dx.doi.org/10.1016/0020-0891(89)90099-7.

[77] Maki AG, Wells JS, Vanek MD. Heterodyne frequency measurements on N_2O near 930 cm^{-1}. J Mol Spectrosc 1989;138:84–8. http://dx.doi.org/10.1016/0022-2852(89)90101-X.

[78] Tang L-W, Nadler S, Daunt SJ. Tunable diode laser measurements of absolute line strengths in the $2\nu_2$ band of N_2O near 8 μm. J Quant Spectrosc Radiat Transfer 1989;41:97–101. http://dx.doi.org/10.1016/0022-4073(89)90131-3.

[79] Varanasi P, Chudamani S. Line strength measurements in the ν_1 fundamental band of $^{14}N_2{}^{16}O$ using a tunable diode laser. J Quant Spectrosc Radiat Transfer 1989;41:359–62. http://dx.doi.org/10.1016/0022-4073(89)90065-4.

[80] Vanek MD, Jennings DA, Wells JS, Maki AG. Frequency measurements of high-J rotational transitions of OCS and N_2O. J Mol Spectrosc 1989;138:79–83. http://dx.doi.org/10.1016/0022-2852(89)90100-8.

[81] Vanek MD, Schneider M, Wells JS, Maki AG. Heterodyne measurements on N_2O near 1635 cm^{-1}. J Mol Spectrosc 1989;134:154–8. http://dx.doi.org/10.1016/0022-2852(89)90137-9.

[82] Yamada KMT. Pure rotation spectrum of NNO in the far infrared region. Z Naturforsch Sect A 1990;45:837–8.

[83] Toth RA. Line-frequency measurements and analysis of N_2O between 900 and 4700 cm^{-1}. Appl Opt 1991;30:5289–315. http://dx.doi.org/10.1364/AO.30.00528.

[84] Maki AG, Wells JS. New wavenumber calibration tables from heterodyne frequency measurements. J Res Natl Inst Stand Technol 1992;97:409–70.

[85] Tan TL, Looi EC, Lua KT. Hot-band spectrum of N_2O near 589 cm^{-1}. J Mol Spectrosc 1992;154:218–22. http://dx.doi.org/10.1016/0022-2852(92)90041-L.

[86] Toth RA. Line strengths (900 – 3600 cm^{-1}), self-broadened linewidths, and frequency-shifts (1800 – 2360 cm^{-1}) of N_2O. Appl Opt 1993;32:7326–65. http://dx.doi.org/10.1364/AO.32.007326.

[87] Sirota JM, Reuter DC. Absolute intensities for the Q-branch of the $3\nu_2-\nu_1$ (465.161 cm^{-1}) band of nitrous oxide. J Quant Spectrosc Radiat Transfer 1993;50:591–4. http://dx.doi.org/10.1016/0022-4073(93)90026-E.

[88] Sirota JM, Reuter DC, Mumma MJ. Blocked impurity band detectors applied to tunable diode laser spectroscopy in the 8- to 28-μm range. Appl Opt 1993;32:2117–21. http://dx.doi.org/10.1364/AO.32.002117.

[89] Rachet F, Margottinmaclou M, Elazizi M, Henry A, Valentin A. Linestrength measurements for N_2O around 4 μm: $\Pi\leftarrow\Sigma$, $\Pi\leftarrow\Pi$, $\Sigma\leftarrow\Pi$, and $\Delta\leftarrow\Pi$ transitions in ($^{14}N_2$ ^{16}O) (2400−2850 cm^{-1}). J Mol Spectrosc 1994;164:196–209. http://dx.doi.org/10.1006/jmsp.1994.1066.

[90] Rachet F, MM, Elazizi M, Henry A, Valentin A. Linestrength measurements for the $30^00\leftarrow02^00$, $10^01\leftarrow01^10$, and $13^10\leftarrow00^00$ transitions of $^{14}N_2{}^{16}O$ (2600-3100 cm^{-1}). J Mol Spectrosc 1994;166:79–87. http://dx.doi.org/10.1006/jmsp.1994.1173.

[91] Elazizi M, Rachet F, Henry A, Margottinmaclou M, Valentin A. Linestrength measurements for N_2O around 4 μm: $\Sigma\leftarrow\Sigma$ transitions in 4 isotopic species (2400 – 2600 cm^{-1}). J Mol Spectrosc 1994;164:180–95. http://dx.doi.org/10.1006/jmsp.1994.1065.

[92] Campargue A, Permogorov D. Intensity measurements of the near-infrared and visible overtone bands of nitrous oxide. Chem Phys Lett 1995;241:339–44. http://dx.doi.org/10.1016/0009-2614(95)00636-I.

[93] Campargue A, Permogorov D, Bach M, Temsamani MA, Vander Auwera J, Herman M, et al. Overtone spectroscopy in nitrous-oxide. J Chem Phys 1995;103:5931–8. http://dx.doi.org/10.1063/1.470473.

[94] Regalia L, Barbe A, Plateaux JJ, Dana V, Mandin JY, Allout MY. Nitrogen-broadening and nitrogen-shifting coefficients in the ν_3 band of N_2O. J Mol Spectrosc 1995;172:563–6. http://dx.doi.org/10.1006/jmsp.1995.1203.

[95] Reuter DC, Sirota JM. Temperature-dependent foreign gas broadening coefficients of the R(42) and P(13) lines in the ν_1 band of N_2O. J Quant Spectrosc Radiat Transfer 1995;54:957–60. http://dx.doi.org/10.1016/0022-4073(95)00127-7.

[96] Willey DR, Ross KA, Mullin AS, Schowen S, Zheng LD, Flynn G. Gas-phase infrared spectroscopy of N_2O in an equilibrium cell at 10-K and 5-K. J Mol Spectrosc 1995;169:66–72. http://dx.doi.org/10.1006/jmsp.1995.1006.

[97] Campargue A. The near-infrared absorption spectrum of nitrous oxide: Analysis of the $5\nu_3$ and $\nu_1+5\nu_3$ clusters. Chem Phys Lett 1996;259:563–7. http://dx.doi.org/10.1016/0009-2614(96)00821-4.

[98] Johns JWC, Lu Z, Weber M, Sirota JM, Reuter DC. Absolute intensities in the ν_2 fundamental of N_2O at 17 μm. J Mol Spectrosc 1996;177:203–10. http://dx.doi.org/10.1006/jmsp.1996.0134.

[99] Margottin-Maclou M, Rachet F, Henry A, Valentin A. Pressure-induced line shifts in the ν_3 band of nitrous oxide perturbed by N_2, O_2, He, Ar and Xe. J Quant Spectrosc Radiat Transfer 1996;56:1–16. http://dx.doi.org/10.1016/0022-4073(96)00029-5.

[100] Tachikawa M, Evenson KM, Zink LR, Maki AG. Frequency measurements of 9- and 10-μm N_2O laser transitions. IEEE J Quant Electr 1996;32:1732–6. http://dx.doi.org/10.1109/3.538777.

[101] Weber M, Sirota JM, Reuter DC. l-Resonance intensity effects and pressure broadening of N_2O at 17 μm. J Mol Spectrosc 1996;177:211–20. http://dx.doi.org/10.1006/jmsp.1996.0135.

[102] Morino I, Fabian M, Takeo H, Yamada KMT. High-J rotational transitions of NNO measured with the NAIR terahertz spectrometer. J Mol Spectrosc 1997;185:142–6. http://dx.doi.org/10.1006/jmsp.1997.7366.

[103] Regalia L, Thomas X, Hamdouni A, Barbe A. Intensities of N_2O measurements in the 4 and 3 μm region using Fourier transform spectrometer. J Quant Spectrosc Radiat Transfer 1997;57:435–44. http://dx.doi.org/10.1016/S0022-4073(96)00160-4.

[104] Bouanich JP, Hartmann JM, Blanquet G, Walrand J, Bermejo D, Domenech JL. Line-mixing effects in He- and N_2-broadened $\Sigma \leftrightarrow \Pi$ infrared Q branches of N_2O. J Chem Phys 1998;109:6684–90. http://dx.doi.org/10.1063/1.477318.

[105] Garnache A, Campargue A, Kachanov AA, Stoeckel F. Intracavity laser absorption spectroscopy near 9400 cm^{-1} with a Nd:glass laser: application to $^{14}N_2{}^{16}O$. Chem Phys Lett 1998;292:698–704. http://dx.doi.org/10.1016/S0009-2614(98)00750-7.

[106] He Y, Hippler M, Quack M. High-resolution cavity ring-down absorption spectroscopy of nitrous oxide and chloroform using a near-infrared CW diode laser. Chem Phys Lett 1998;289:527–34. http://dx.doi.org/10.1016/S0009-2614(98)00424-2.

[107] Hippler M, Quack M. CW cavity ring-down infrared absorption spectroscopy in pulsed supersonic jets: Nitrous oxide and methane. Chem Phys Lett 1999;314:273–81. http://dx.doi.org/10.1016/S0009-2614(99)01071-4.

[108] Morino I, Yamada KMT, Maki AG. Terahertz measurements of rotational transitions in vibrationally excited states of N_2O. J Mol Spectrosc 1999;196:131–8. http://dx.doi.org/10.1006/jmsp.1999.7855.

[109] Oshika H, Toba A, Fujitake M, Ohashi N. Newly observed vibrotational bands of N_2O in 1.3 μm region. J Mol Spectrosc 1999;197:324–5. http://dx.doi.org/10.1006/jmsp.1999.7922.

[110] Toth RA. Line positions and strengths of N_2O between 3515 and 7800 cm^{-1}. J Mol Spectrosc 1999;197:158–87. http://dx.doi.org/10.1006/jmsp.1999.7907.

[111] Weirauch G, Kachanov AA, Campargue A, Bach M, Herman M, Vander Auwera J. Refined investigation of the overtone spectrum of nitrous oxide. J Mol Spectrosc 2000;202:98–106. http://dx.doi.org/10.1006/jmsp.2000.8114.

[112] Toth RA. N_2- and air-broadened linewidths and frequency-shifts of N_2O. J Quant Spectrosc Radiat Transfer 2000;66:285–304. http://dx.doi.org/10.1016/S0022-4073(99)00167-3.

[113] Bailly D, Vervloet M. $^{14}N_2$ ^{16}O in emission in the 4.5 μm region: Transitions $v_1v_2^lv_3 \rightarrow v_1v_2^l(v_3-1)$ occurring between highly excited vibrational states. J Mol Spectrosc 2001;209:207–15. http://dx.doi.org/10.1006/jmsp.2001.8420.

[114] Campargue A, Weirauch G, Tashkun SA, Perevalov VI, Teffo JL. Overtone spectroscopy of N_2O between 10 000 and 12 000 cm^{-1}: A test of the polyad approach. J Mol Spectrosc 2001;209:198–206. http://dx.doi.org/10.1006/jmsp.2001.8414.

[115] Daumont L, Vander Auwera J, Teffo JL, Perevalov VI, Tashkun SA. Line intensity measurements in $^{14}N_2{}^{16}O$ and their treatment using the effective dipole moment approach. J Mol Spectrosc 2001;208:281–91. http://dx.doi.org/10.1006/jmsp.2001.8400.

[116] Bertseva E, Kachanov AA, Campargue A. Intracavity laser absorption spectroscopy of N_2O with a vertical external cavity surface emitting laser. Chem Phys Lett 2002;351:18–26. http://dx.doi.org/10.1016/S0009-2614(01)01321-5.

[117] Daumont L, Claveau C, Debacker-Barilly MR, Hamdouni A, Regalia-Jarlot L, Teffo JL, et al. Line intensities of $^{14}N_2{}^{16}O$: The 10 micrometers region revisited. J Quant Spectrosc Radiat Transff 2002;72:37–55. http://dx.doi.org/10.1016/S0022-4073(01)00054-1.

[118] Bailly D, Pirali O, Vervloet M. $^{14}N_2$ ^{16}O emission in the 4.5 μm region: High excitation of the bending mode transitions $v_1v_2^lv_3 \rightarrow v_1v_2^lv_3-1$ with $(2v_1+v_2)=5$. J Mol Spectrosc 2003;222:180–90. http://dx.doi.org/10.1016/S0022-2852(03)00179-6.

[119] Ding Y, Perevalov VI, Tashkun SA, Teffo JL, Hu S, Bertseva E, et al. Weak overtone transitions of N_2O around 1.05 μm by ICLAS-VECSEL. J Mol Spectrosc 2003;220:80–6. http://dx.doi.org/10.1016/S0022-2852(03)00060-2.

[120] Morino I, Yamada KMT. Absorption line profiles of N_2O measured for the $J=25-24$ and $26-25$ rotational transitions. J Mol Spectrosc 2003;219:282–9. http://dx.doi.org/10.1016/S0022-2852(03)00030-4.

[121] Parkes AM, Linsley AR, Orr-Ewing AJ. Absorption cross-sections and pressure broadening of rotational lines in the $3\nu_3$ band of N_2O determined by diode laser cavity ring-down spectroscopy. Chem Phys Lett 2003;377:439–44. http://dx.doi.org/10.1016/S0009-2614(03)01155-2.

[122] Rohart F, Colmont JM, Wlodarczak G, Bouanich JP. N_2- and O_2-broadening coefficients and profiles for millimeter lines of $^{14}N_2O$. J Mol Spectrosc 2003;222:159–71. http://dx.doi.org/10.1016/S0022-2852(03)00220-0.

[123] Bertseva E, Campargue A, Perevalov VI, Tashkun SA. New observations of weak overtone transitions of N_2O by ICLAS-VeCSEL near 1.07 μm. J Mol Spectrosc 2004;226:196–200. http://dx.doi.org/10.1016/j.jms.2004.03.021.

[124] Nemtchinov V, Sun CB, Varanasi P. Measurements of line intensities and line widths in the ν_3-fundamental band of nitrous oxide at atmospheric temperatures. J Quant Spectrosc Radiat Transfer 2004;83:267–84. http://dx.doi.org/10.1016/S0022-4073(02)00355-2.

[125] Toth RA. Linelist of N_2O Parameters from 500 to 7500 cm^{-1}. Tech. Rep. JPL, 2004, https://mark4sun.jpl.nasa.gov/n2o.html.

[126] Vitcu A, Ciurylo R, Wehr R, Drummond JR, May AD. Broadening, shifting, and line mixing in the $03^10 \leftarrow 01^10$ parallel Q branch of N_2O. J Mol Spectrosc 2004;226:71–80. http://dx.doi.org/10.1016/j.jms.2004.03.017.

[127] Drouin BJ, Maiwald FW. Extended THz measurements of nitrous oxide, N_2O. J Mol Spectrosc 2006;236:260–2. http://dx.doi.org/10.1016/j.jms.2006.01.005.

[128] Herbin H, Picque N, Guelachvili G, Sorokin E, Sorokina IT. N_2O weak lines observed between 3900 and 4050 cm^{-1} from long path absorption spectra. J Mol Spectrosc 2006;238:256–9. http://dx.doi.org/10.1016/j.jms.2006.05.004.

[129] Wang L, Perevalov VI, Tashkun SA, Gao B, Hao LY, Hu SM. Fourier transform spectroscopy of N_2O weak overtone transitions in the 1-2 μm region. J Mol Spectrosc 2006;237:129–36. http://dx.doi.org/10.1016/j.jms.2006.03.007.

[130] Daumont L, Vander Auwera J, Teffo J-L, Perevalov VI, Tashkun SA. Line intensity measurements in $^{14}N_2{}^{16}O$ and their treatment using the effective dipole moment approach. II. The 5400-11000 cm^{-1} region. J Quant Spectrosc Radiat Transfer 2007;104:342–56. http://dx.doi.org/10.1016/j.jqsrt.2006.09.004.

[131] Didriche K, Macko P, Herman M, Thievin J, Benidar A, Georges R. Investigation of the shape of the R(0) absorption line in ν_3, N_2O recorded from an axisymmetric supersonic free jet expansion. J Quant Spectrosc Radiat Transf 2007;105:128–38. http://dx.doi.org/10.1016/j.jqsrt.2006.10.002.

[132] Horneman V-M. High accurate peak positions for calibration purposes with the lowest fundamental bands ν_2 of N_2O and CO_2. J Mol Spectrosc 2007;241:45–50. http://dx.doi.org/10.1016/j.jms.2006.10.014.

[133] Liu AW, Kassi S, Malara P, Romanini D, Perevalov VI, Tashkun SA, et al. High sensitivity CW-cavity ring down spectroscopy of N_2O near 1.5 μm (I). J Mol Spectrosc 2007;244:33–47. http://dx.doi.org/10.1016/j.jms.2007.01.007.

[134] Liu AW, Kassi S, Perevalov VI, Tashkun SA, Campargue A. High sensitivity CW-cavity ring down spectroscopy of N_2O near 1.5 μm (II). J Quant Spectrosc Radiat Transfer 2007;244:48–62. http://dx.doi.org/10.1016/j.jms.2007.05.010.

[135] Nakayama T, Fukuda H, Sugita A, Hashimoto S, Kawasaki M, Aloisio S, et al. Buffer-gas pressure broadening for the $(00(0)3) \leftarrow (00(0)0)$ band of N_2O measured with continuous-wave cavity ring-down spectroscopy. Chem Phys 2007;334:196–203. http://dx.doi.org/10.1016/j.chemphys.2007.03.001.

[136] Liu AW, Kassi S, Perevalov VI, Hu SM, Campargue A. High sensitivity CW-cavity ring down spectroscopy of N_2O near 1.5 μm (III). J Mol Spectrosc 2009;254:20–7. http://dx.doi.org/10.1016/j.jms.2008.12.006.

[137] Sun H, Ding YJ, Zotova IB. Differentiation of three isotopic variants of nitrous oxide based on spectra of rotational transitions. In: 2009 Conference on Lasers and Electro-Optics and Quantum Electronics and Laser Science Conference, VOLS 1-5. CLEO/QELS 2009, OSA; 2009, p. 2913. http://dx.doi.org/10.1364/CLEO.2009.JTuD80, +.

[138] Wang CY, Liu AW, Perevalov VI, Tashkun SA, Song KF, Hu SM. High-resolution infrared spectroscopy of $^{14}N^{15}N^{16}O$ and $^{15}N^{14}N^{16}O$ in the 1200–3500 cm^{-1} region. J Mol Spectrosc 2009;257:94–104. http://dx.doi.org/10.1016/j.jms.2009.06.012.

[139] Aenchbacher W, Naftaly M, Dudley R. Line strengths and self-broadening of pure rotational lines of nitrous oxide measured by terahertz time-domain spectroscopy. J Opt Soc Amer B 2010;27:1717–21. http://dx.doi.org/10.1364/JOSAB.27.001717.

[140] Liu AW, Kassi S, Perevalov VI, Tashkun SA, Campargue A. High sensitivity cw-cavity ring down spectroscopy of N_2O near 1.28 μm. J Mol Spectrosc 2011;267:191–9. http://dx.doi.org/10.1016/j.jms.2011.03.025.

[141] Milloud R, Perevalov VI, Tashkun SA, Campargue A. Rotational analysis of $6\nu_3$ and $6\nu_3+\nu_2-\nu_2$ bands of $^{14}N_2{}^{16}O$ from ICLAS spectra between 12 760 and 12 900 cm^{-1}. J Quant Spectrosc Radiat Transfer 2011;112:553–7. http://dx.doi.org/10.1016/j.jqsrt.2010.10.013.

[142] Lu Y, Mondelain D, Liu AW, Perevalov VI, Kassi S, Campargue A. High sensitivity CW-cavity ring down spectroscopy of N_2O between 6950 and 7653 cm^{-1} (1.44–1.31 μm): I. line positions. J Quant Spectrosc Radiat Transf 2012;113:749–62. http://dx.doi.org/10.1016/j.jqsrt.2012.03.005.

[143] Perevalov VI, Tashkun SA, Kochanov RV, Liu AW, Campargue A. Global modeling of the $^{14}N_2{}^{16}O$ line positions within the framework of the polyad model of effective Hamiltonian. J Quant Spectrosc Radiat Transfer 2012;113:1004–12. http://dx.doi.org/10.1016/j.jqsrt.2011.12.008.

[144] Karlovets EV, Lu Y, Mondelain D, Kassi S, Campargue A, Tashkun SA, et al. High sensitivity CW-cavity ring down spectroscopy of N_2O between 6950 and 7653 cm^{-1} (1.44-1.31 μm): II. Line intensities. J Quant Spectrosc Radiat Transf 2013;117:81–7. http://dx.doi.org/10.1016/j.jqsrt.2012.11.003.

[145] Knabe K, Williams PA, Giorgetta FR, Radunsky MB, Armacost CM, Crivello S, et al. Absolute spectroscopy of N_2O near 4.5 μm with a comb-calibrated, frequency-swept quantum cascade laser spectrometer. Opt Expr 2013;21:1020–9. http://dx.doi.org/10.1364/OE.21.001020.

[146] Ting W-J, Chang C-H, Chen S-E, Chen H-C, Shy J-T, Drouin BJ, et al. Precision frequency measurement of N_2O transitions near 4.5 μm and above 150 μm. J Opt Soc Amer 2014;31:1954–63. http://dx.doi.org/10.1364/JOSAB.31.001954.

[147] Wu Z-W, Dong Y-T, Zhou W-D. Near infrared cavity enhanced absorption spectroscopy study of N_2O. Spectrosc Spect Anal 2014;34:2081–4.

[148] Gambetta A, Cassinerio M, Coluccelli N, Fasci E, Castrillo A, Gianfrani L, et al. Direct phase-locking of a 8.6-μm quantum cascade laser to a mid-IR optical frequency comb: application to precision spectroscopy of N_2O. Opt Lett 2015;40:304–7. http://dx.doi.org/10.1364/OL.40.000304.

[149] Loos J, Birk M, Wagner G. Pressure broadening, -shift, speed dependence and line mixing in the υ_3 rovibrational band of N_2O. J Quant Spectrosc Radiat Transfer 2015;151:300–9. http://dx.doi.org/10.1016/j.jqsrt.2014.10.008.

[150] Karlovets EV, Campargue A, Kassi S, Perevalov VI, Tashkun SA. High sensitivity cavity ring down spectroscopy of N_2O near 1.22 μm: (I) Rovibrational assignments and band-by-band analysis. J Quant Spectrosc Radiat Transfer 2016;169:36–48. http://dx.doi.org/10.1016/j.jqsrt.2015.09.012.

[151] Tashkun SA, Perevalov VI, Lavrentieva NN. NOSD-1000, the high-temperature nitrous oxide spectroscopic databank. J Quant Spectrosc Radiat Transff 2016;177:43–8. http://dx.doi.org/10.1016/j.jqsrt.2015.11.014.

[152] Tonokura K, Takahashi R. Pressure broadening of the ν_1 band of nitrous oxide by carbon dioxide. Chem Lett 2016;45:95–7. http://dx.doi.org/10.1246/cl.150932.

[153] Werwein V, Brunzendorf J, Serdyukov A, Werhahn O, Ebert V. First measurements of nitrous oxide self-broadening and self-shift coefficients in the 0002-0000 band at 2.26 μm using high resolution Fourier transform spectroscopy. J Mol Spectrosc 2016;323:28–42. http://dx.doi.org/10.1016/j.jms.2016.01.010.

[154] Werwein V, Brunzendorf J, Li G, Serdyukov A, Werhahn O, Ebert V. High-resolution Fourier transform measurements of line strengths in the $00^02 - 00^00$ main isotopologue band of nitrous oxide. Appl Opt 2017;56:E99–105. http://dx.doi.org/10.1364/AO.56.000E99.

[155] Zhao X-Q, Wang J, Liu A-W, Zhou Z-Y, Hu S-M. High precision cavity ring down spectroscopy of $6\nu_3$ overtone band of $^{14}N_2{}^{16}O$ near 775 nm. Chin J Chem Phys 2017;30:487–92. http://dx.doi.org/10.1063/1674-0068/30/cjcp1705109.

[156] AlSaif B, Lamperti M, Gatti D, Laporta P, Fermann M, Farooq A, et al. High accuracy line positions of the υ_1 fundamental band of $^{14}N_2{}^{16}O$. J Quant Spectrosc Radiat Transfer 2018;211:172–8. http://dx.doi.org/10.1016/j.jqsrt.2018.03.005.

[157] Lauzin C, Schmutz H, Agner JA, Merkt F. Chirped-pulse millimetre-wave spectrometer for the 140-180 GHz region. Mol Phys 2018;116:3656–65. http://dx.doi.org/10.1080/00268976.2018.1467055.

[158] Bertin T, Mondelain D, Karlovets E, Kassi S, Perevalov V, Campargue A. High sensitivity cavity ring down spectroscopy of N_2O near 1.74 μm. J Quant Spectrosc Radiat Transfer 2019;229:40–9. http://dx.doi.org/10.1016/j.jqsrt.2019.02.011.

[159] Liu GL, Wang J, Tan Y, Kang P, Bi Z, Liu AW, et al. Line positions and N_2-induced line parameters of the $00^03 - 00^00$ band of $^{14}N_2{}^{16}O$ by comb-assisted cavity ring-down spectroscopy. J Quant Spectrosc Radiat Transfer 2019;229:17–22. http://dx.doi.org/10.1016/j.jqsrt.2019.03.004.

[160] Tashkun SA. Global modeling of the $^{14}N_2{}^{16}O$ line positions within the framework of the non-polyad model of effective Hamiltonian. J Quant Spectrosc Radiat Transfer 2019;231:88–101. http://dx.doi.org/10.1016/j.jqsrt.2019.04.023.

[161] Kim G-R, Lee H-B, Jeon T-I. Terahertz time-domain spectroscopy of low-concentration N_2O using long-range multipass gas cell. IEEE Trans Terahertz Sci Technol 2020;10:524–30. http://dx.doi.org/10.1109/TTHZ.2020.2997601.

[162] Odintsova TA, Fasci E, Gravina S, Gianfrani L, Castrillo A. Optical feedback laser absorption spectroscopy of N_2O at 2 μm. J Quant Spectrosc Radiat Transfer 2020;254:107190. http://dx.doi.org/10.1016/j.jqsrt.2020.107190.

[163] Bailey DM, Zhao G, Fleisher AJ. Precision spectroscopy of N_2O with a cross-dispersed spectrometer and mid-infrared frequency comb. In: 2020 Conference on Lasers and Electro-Optics (CLEO), Conference on Lasers and Electro-Optics. OSA; 2020.

[164] Zhao G, Bailey DM, Fleisher AJ, Hodges JT, Lehmann KK. Doppler-free two-photon cavity ring-down spectroscopy of a nitrous oxide (N_2O) vibrational overtone transition. Phys Rev A 2020;101:062509. http://dx.doi.org/10.1103/PhysRevA.101.062509.

[165] Ogden HM, Michael TJ, Murray MJ, Mullin AS. Transient IR (0001–0000) absorption spectroscopy of optically centrifuged N_2O with extreme rotation up to $J = 205$. J Quant Spectrosc Radiat Transfer 2020;246:106867. http://dx.doi.org/10.1016/j.jqsrt.2020.106867.

[166] Adkins EM, Long DA, Fleisher AJ, Hodges JT. Near-infrared cavity ring-down spectroscopy measurements of nitrous oxide in the (4200) ← (0000) and (5000) ← (0000) bands. J Quant Spectrosc Radiat Transfer 2021;262:107527. http://dx.doi.org/10.1016/j.jqsrt.2021.107527.

[167] Hashemi R, Gordon IE, Adkins EM, Hodges JT, Long DA, Birk M, et al. Improvement of the spectroscopic parameters of the air- and self-broadened N_2O and CO lines for the HITRAN2020 database applications. J Quant Spectrosc Radiat Transfer 2021;271:107735. http://dx.doi.org/10.1016/j.jqsrt.2021.107735.

[168] Hjalten A, Germann M, Krzempek K, Hudzikowski A, Gluszek A, Tomaszewska D, et al. Optical frequency comb Fourier transform spectroscopy of $^{14}N_2{}^{16}O$ at 7.8 μm. J Quant Spectrosc Radiat Transfer 2021;271:107734. http://dx.doi.org/10.1016/j.jqsrt.2021.107734.

[169] Jiang J, McCartt AD. Two-color, intracavity pump–probe, cavity ringdown spectroscopy. J Chem Phys 2021;155:104201. http://dx.doi.org/10.1063/5.0054792.

[170] Karlovets EV, Kassi S, Tashkun SA, Campargue A. The absorption spectrum of nitrous oxide between 8325 and 8622 cm^{-1}. J Quant Spectrosc Radiat Transfer 2021;262:107508. http://dx.doi.org/10.1016/j.jqsrt.2021.107508.

[171] Lepère M, Browet O, Clément J, Vispoel B, Allmendinger P, Hayden J, et al. A mid-infrared dual-comb spectrometer in step-sweep mode for high-resolution molecular spectroscopy. J Quant Spectrosc Radiat Transfer 2022;287:108239. http://dx.doi.org/10.1016/j.jqsrt.2022.108239.

[172] Zhao G, Tian J, Hodges JT, Fleisher AJ. Frequency stabilization of a quantum cascade laser by weak resonant feedback from a fabry–perot cavity. Opt Lett 2021;46:3057–60. http://dx.doi.org/10.1364/OL.427083.

[173] Iwakuni K. Absolute frequency measurement of the $3\nu_1$ band of N_2O with comb-locked rapid scan spectroscopy using a multi-pass cell. J Mol Spectrosc 2022;384:111571. http://dx.doi.org/10.1016/j.jms.2022.111571.

[174] Karlovets EV, Tashkun SA, Kassi S, Campargue A. An improved analysis of the N_2O absorption spectrum in the 1.18 μm window. J Quant Spectrosc Radiat Transfer 2022;278:108003. http://dx.doi.org/10.1016/j.jqsrt.2021.108003.

[175] Karlovets EV, Kassi S, Tashkun SA, Campargue A. The absorption spectrum of nitrous oxide between 7647 and 7918 cm^{-1}. J Quant Spectrosc Radiat Transfer 2022;108199. http://dx.doi.org/10.1016/j.jqsrt.2022.108199.

[176] Lucchesini A, Gonzalez-Rivera J. Nitrous oxide spectroscopy at 887 nm. J Quant Spectrosc Radiat Transfer 2022;283:108140. http://dx.doi.org/10.1016/j.jqsrt.2022.108140.

[177] Huang X, Schwenke DW, Lee TJ. Highly accurate potential energy surface and dipole moment surface for nitrous oxide and 296 K infrared line list for $^{14}N_2{}^{16}O$. Mol Phys 2023;e2232892. http://dx.doi.org/10.1080/00268976.2023.2232892.

[178] Karlovets EV, Mondelain D, Tashkun SA, Campargue A. The absorption spectrum of nitrous oxide between 7250 and 7653 cm^{-1}. J Quant Spectrosc Radiat Transfer 2023;301:108511. http://dx.doi.org/10.1016/j.jqsrt.2023.108511.

[179] Tashkun SA, Campargue A. The NOSL-296 high resolution $^{14}N_2{}^{16}O$ line list for atmospheric applications. J Quant Spectrosc Radiat Transfer 2023;295:108417. http://dx.doi.org/10.1016/j.jqsrt.2022.108417.

[180] Sinitsa LN, Serdyukov VI, Emelyanov NM, Marinina AA, Perevalov VI. LED-based Fourier transform spectroscopy of $^{14}N_2{}^{16}O$ in the 9750-12000 cm^{-1} region. J Quant Spectrosc Radiat Transfer 2024;315:108888. http://dx.doi.org/10.1016/j.jqsrt.2023.108888.

[181] Hargreaves RJ, Gordon IE, Rothman LS, Tashkun SA, Perevalov VI, Lukashevskaya AA, et al. Spectroscopic line parameters of NO, NO_2, and N_2O for the HITEMP database. J Quant Spectrosc Radiat Transf 2019;232:35–53. http://dx.doi.org/10.1016/j.jqsrt.2019.04.040.

[182] Gordon IE, Rothman LS, Hargreaves RJ, Hashemi R, Karlovets EV, Skinner FM, et al. The HITRAN2020 molecular spectroscopic database. J Quant Spectrosc Radiat Transf 2022;277:107949. http://dx.doi.org/10.1016/j.jqsrt.2021.107949.

[183] Suzuki I. General anharmonic force constants of nitrous oxide. J Mol Spectrosc 1969;32:54–73. http://dx.doi.org/10.1016/0022-2852(69)90142-8.

[184] Chedin A, Amiot C, Cihla Z. The potential energy function of the nitrous oxide molecule using pure vibrational data. J Mol Spectrosc 1976;63:348–69. http://dx.doi.org/10.1016/0022-2852(76)90302-7.

[185] Lacy M, Whiffen D. The anharmonic force field of nitrous oxide. Mol Phys 1982;45:241–52. http://dx.doi.org/10.1080/00268978200100191.

[186] Kobayashi M, Suzuki I. Sextic force field of nitrous oxide. J Mol Spectrosc 1987;125:24–42. http://dx.doi.org/10.1016/0022-2852(87)90190-1.

[187] Teffo J-L, Chédin A. Internuclear potential and equilibrium structure of the nitrous oxide molecule from rovibrational data. J Mol Spectrosc 1989;135:389–409. http://dx.doi.org/10.1016/0022-2852(89)90164-1.

[188] Allen WD, Yamaguchi Y, Császár AG, Clabo Jr DA, Remington RB, Schaefer III HF. A systematic study of molecular vibrational anharmonicity and vibration–rotation interaction by self-consistent-field higher derivative methods. Linear polyatomic molecules. Chem Phys 1990;145:427–66. http://dx.doi.org/10.1016/0301-0104(90)87051-C.

[189] Császár AG. Anharmonic force field of N_2O. J Phys Chem 1994;98:8823–6. http://dx.doi.org/10.1021/j100087a001.
[190] Zúñiga J, Bastida A, Requena A. Theoretical calculations of vibrational frequencies and rotational constants of the N_2O isotopomers. J Mol Spectrosc 2003;217:43–58. http://dx.doi.org/10.1016/S0022-2852(02)00014-0.
[191] Czakó G, Furtenbacher T, Császár AG, Szalay V. Variational vibrational calculations using high-order anharmonic force fields. Mol Phys 2004;102:2411–23. http://dx.doi.org/10.1080/00268970420002749 91.
[192] Acharjee M, Choudhury J, Sen R, Mohanta B. The vibrational spectra of carbon dioxide and nitrous oxide: A Lie algebraic study. Can J Phys 2018;96:560–5. http://dx.doi.org/10.1139/cjp-2017-0387.
[193] Császár AG, Furtenbacher T. Spectroscopic networks. J Mol Spectrosc 2011;266:99–103. http://dx.doi.org/10.1016/j.jms.2011.03.031.
[194] Furtenbacher T, Árendás P, Mellau G, Császár AG. Simple molecules as complex systems. Sci Rep 2014;4:4654. http://dx.doi.org/10.1038/srep04654.
[195] Császár AG, Furtenbacher T, Arendas P. Small molecules – Big data. J Phys Chem A 2016;120:8949–69. http://dx.doi.org/10.1021/acs.jpca.6b02293.
[196] Császár AG, Czakó G, Furtenbacher T, Mátyus E. An active database approach to complete rotational–vibrational spectra of small molecules. Annu Rep Comput Chem 2007;3:155–76. http://dx.doi.org/10.1016/S1574-1400(07)03009-5.
[197] Furtenbacher T, Császár AG. MARVEL: measured active rotational-vibrational energy levels. II. Algorithmic improvements. J Quant Spectrosc Radiat Transf 2012;113:929–35. http://dx.doi.org/10.1016/j.jqsrt.2012.01.005.
[198] E.B. Wilson Jr, Decius JC, Cross PC. Molecular vibrations: The theory of infrared and Raman vibrational spectra. New York: McGraw Hill; 1955.
[199] Teffo JL, Perevalov VI, Lyulin OM. Reduced effective Hamiltonian for a global treatment of rovibrational energy levels of nitrous oxide. J Mol Spectrosc 1994;168:390–403. http://dx.doi.org/10.1006/jmsp.1994.1288.
[200] Waalkens H, Jung C, Taylor HS. Semiclassical assignment of the vibrational spectrum of N_2O. J Phys Chem A 2002;106:911–24. http://dx.doi.org/10.1021/jp013057w.
[201] Mizus II, Zobov NF, Makhnev VY, Ovsyannikov RI, Rogov MA, Tennyson J, Polyansky OL. Approaching experimental accuracy for triatomic spectra using variational calculations: Potential energy and dipole moment surfaces of N_2O. J Quant Spectrosc Radiat Transf 2024. [in preparation].
[202] Efron B. Bootstrap methods: Another look at the jackknife. Ann Statist 1979;7. http://dx.doi.org/10.1214/aos/1176344552.
[203] Hastie T, Tibshirani R, Friedman J. The elements of statistical learning. 2nd ed.. Springer New York; 2009, http://dx.doi.org/10.1007/978-0-387-84858-7.
[204] Tóbiás R, Furtenbacher T, Tennyson J, Császár AG. Accurate empirical rovibrational energies and transitions of $H_2{}^{16}O$. Phys Chem Chem Phys 2019;21:3473–95. http://dx.doi.org/10.1039/c8cp05169k.
[205] Watson JKG. Robust weighting in least-square fits. J Mol Spectrosc 2003;219:326–8. http://dx.doi.org/10.1016/S0022-2852(03)00100-0.
[206] Tóbiás R, Furtenbacher T, Simkó I, Császár AG, Diouf ML, Cozijn FMJ, et al. Spectroscopic-network-assisted precision spectroscopy and its application to water. Nature Commun 2020;11:1708. http://dx.doi.org/10.1038/s41467-020-15430-6.
[207] Diouf ML, Tóbiás R, Simkó I, Cozijn FMJ, Salumbides EJ, Ubachs W, et al. Network-based design of near-infrared Lamb-dip experiments and the determination of pure rotational energies of $H_2{}^{18}O$ at kHz accuracy. J Phys Chem Ref Data 2021;50:023106. http://dx.doi.org/10.1063/5.0052744.
[208] Castrillo A, Fasci E, Furtenbacher T, D'Agostino V, Khan MA, Gravina S, et al. On the $^{12}C_2H_2$ near-infrared spectrum: absolute transition frequencies and an improved spectroscopic network at the kHz accuracy level. Phys Chem Chem Phys 2023;25:23614–25. http://dx.doi.org/10.1039/d3cp01835k.
[209] Brown JM, Hougen JT, Huber KP, Johns JWC, Kopp I, Lefebvre-Brion H, et al. Labeling of parity doublet levels in linear molecules. J Mol Spectrosc 1975;55:500–3. http://dx.doi.org/10.1016/0022-2852(75)90291-X.
[210] Lovas FJ. Microwave spectral tables II. Triatomic molecules. J Phys Chem Ref Data 1978;7:1445–750. http://dx.doi.org/10.1063/1.555588.